

Status of Implementation of SHRP2 Specifications to the AASHTO LRFD: Recommendations from *Service Limit State Design for Bridges*

This brief report summarizes the service limit states investigated in the second Strategic Highway Research Program (SHRP2) project, *Service Limit State Design for Bridges* (R19B), and their implementation status as of March 2017. The agenda items attached to this report show the proposed revisions as they appeared in the annual meeting agenda of the 2015 and 2016 American Association of State Highway and Transportation Officials (AASHTO) Subcommittee on Bridges and Structures (SCOBS). The meetings were held on April 20 to 23, 2015, in Saratoga Springs, New York, and on June 27 to 30, 2016, in Minneapolis, Minnesota, respectively. The final revisions may be slightly different due to minor changes that may have been approved during the meeting. In order to ensure that any revisions be understood and considered for implementation beyond the initial states engaged in implementing *Service Limit State Design*, it is recommended that additional training for the broader bridge engineering community be considered. This training would best be accomplished via multiple webinars covering the topics of Live-Load Calibration, Service Limit States and Geotechnical/Foundations.

Service III Load Combination: Cracking of Prestressed Concrete

Service Limit State Design for Bridges and the National Cooperative Highway Research Program (NCHRP) 12-83 project recommended revisions to the load factor for live load for the Service III load combination. Instead of using a 0.8 load factor for all cases, the recommended load factor is dependent on the method used to estimate prestressing losses. The recommended load factors are 1.0 or 0.8. See Attachment 1 for the agenda item.

Status: The proposed revisions were adopted during the 2015 SCOBS annual meeting.

Future implementation work suggested: Training is recommended for the broader bridge engineering community regarding the background and history of the limit state.

Fatigue Limit State

An agenda item, including several revisions related to the fatigue limit state in the AASHTO load and resistance factor design (LRFD), was included in the agenda for the 2015 SCOBS annual meeting. Following are the AASHTO LRFD proposed revisions in the agenda item:

- An increase in the live load factor for Fatigue I from 1.5 to 2.0 and for Fatigue II from 0.75 to 0.8.

- Some revisions associated with the increase in load factor (e.g., the table for average daily truck traffic [ADTT] beyond which infinite fatigue life should be considered).
- Revisions to the table for number of load cycles per truck passage.
- Revisions to the equations for fatigue of reinforcement in reinforced concrete.

The original recommendations of *Service Limit State Design* also included revisions to the fatigue S-N curves for some fatigue categories for structural steel details. These recommendations were not included in the agenda item due to the desire of the AASHTO SCOBS Technical Committee on Structural Steel Design (T14) to keep the existing curves that match those used by the American Institute of Steel (AISC).

Please see Attachment 2 for the 2015 agenda item. The agenda item was withdrawn during the meeting due to concerns that the 2.0 load factor for live load for Fatigue I is too high. More specifically, the concern is that the higher factor will cause some fatigue categories to control the design where they previously did not control the design.

Additional research was performed and resulted in recommending the load factor for Fatigue I to be 1.75 (instead of 1.5 currently in the specifications and 2.0 originally recommended by *Service Limit State Design*).

Status: An agenda item has been included for the 2016 SCOBS annual meeting that is similar to the 2015 item except that the proposed load factor for live load for Fatigue I is 1.75. The agenda item was balloted and it will be incorporated in the AASHTO LRFD.

See Attachment 3 for the proposed 2016 agenda item covering the revisions to the Fatigue Limit State.

Future implementation work suggested: Training for the broader bridge engineering community is recommended for the following areas:

- Background of the revisions to the fatigue provisions.
- Background of the original recommendation for changing the S-N curves for some structural steel fatigue categories to produce uniform reliability.
- Background of the recommendation to revise the equations for fatigue of reinforcement in reinforced concrete to produce uniform reliability.

Service I: Control of Cracking of Reinforced Concrete Components through the Distribution of Reinforcement

The research indicated that the current specification provisions produce uniform reliability. In the absence of reasons to increase or decrease the level of reliability index produced by these

provisions, it was concluded that revisions to these provisions are not needed at this time. No revisions to the specifications were recommended.

Future implementation work suggested: Training for the broader bridge engineering community is recommended regarding the background of the specification requirements to allow future revisions when further research determines whether the current level of reliability is the correct one or whether changing the level of reliability is needed.

Service I: Deflection

The research indicated that there were no widely accepted criteria on dynamic response to live load. The criterion used by the CAN/CSA S6 Canadian Bridge Design Code was investigated. This criterion is based on varying the allowed static deflection based on the first natural frequency of the structure—not the span length as in AASHTO LRFD. The research indicated that the deflection limits in AASHTO produce the same trend as is produced by the CSA provisions.

Status: During the 2015 SCOBS annual meeting, the subcommittee voted to include commentary to the deflection provisions to indicate that other criteria based on deflection-frequency-perception requirements exist and made a reference to the *Service Limit State Design* report. See Attachment 4 for the 2015 agenda item.

Future implementation work suggested: Training for the broader bridge engineering community is needed regarding the deflection-frequency-perception requirements. This will decrease the concern regarding changing the long-used deflection criteria for a more rational criteria based on frequency and accelerations in the future.

Service I: Foundations Deformations

The calibration of foundations deformations is the topic of a paper produced under the *Service Limit State Design* implementation effort. For further details, see *Incorporation of Foundation Deformations in AASHTO LRFD Bridge Design Process*, available at http://shrp2.transportation.org/Pages/R19B_ServiceLimitStateDesignforBridges.aspx.

This work produced new concepts and represents pioneering work. To allow ease of application, the proposed specification revisions were developed such that the general conventional processes used in determining foundation deformations are also used in the proposed revisions.

Status: The Agenda item was not presented to the full SCOBS in 2015. Following the 2015 SCOBS meeting, the agenda item was updated and it was the subject of several discussions between T-15, AASHTO SCOBS Technical Committee on Loads (T-5), and the SHRP2 R19B team. Following the update, an agenda item was proposed for the 2016 SCOBS annual meeting. The item did not ballot and the AASHTO SCOBS Technical Committee on Substructures and Retaining Walls (T-15)

asked for additional information. The agenda item was revised for discussion at the T-15 2016 mid-year committee meeting. See Attachment 5 for the revised agenda item as of November 2016. It is unknown if the agenda items will be balloted in 2017 or in a future year.

Future implementation work suggested: An additional white paper has been requested to document the database evaluated in 2016 for the effects that the proposed agenda item would have on the data. This database included data provided by Tony Allen, chair of T-15, based on WSDOT projects. In addition, work with T-15 is needed to finalize the agenda item and the presentation to SCOBS. Finally, a major training effort for the broader bridge engineering community is needed regarding the new concepts introduced by the research and the proposed revisions. This training will ease the concerns that usually surrounds the introduction of new concepts and will increase the chances of SCOBS voting for the proposed revisions.

Service II Load Combination: Premature Yielding of Steel Structures

The validity of the existing load factor for the Service II load combination was investigated in *Service Limit State Design*. The research suggested that the current load factor is justifiable given the limited background of this limit state. The research also suggested that it may be possible to use the distribution factors for a single lane loaded for this limit state except for areas with heavy truck traffic. Discussions with some members of AASHTO technical committees indicated that using the distribution factor for one lane will not be desirable particularly with the current drive to increase the legal loads. See Attachment 6 for the agenda item.

Status: SCOBS approved an agenda item that included additions to the description of the limit state and the commentary. See Attachment 6 for the agenda item.

Future implementation work suggested: Training for the broader bridge engineering community is needed regarding the background of the limit state and the research as well as for recognizing the situations that may require considering site-specific conditions.

ATTACHMENT 1

Service III, Tension in Prestressed Components, Agenda Item
From
the 2015 SCOBS Annual Meeting Agenda

2015 AASHTO BRIDGE COMMITTEE AGENDA ITEM: 4

SUBJECT: LRFD Bridge Design Specifications: Section 3, Articles 3.4.1 and 3.16
The Manual for Bridge Evaluation: Section 6, Tables 6A.4.2.2-1 and 6A.4.2.2-2;
Appendix B6A, Tables B6A-1 and B6A-2 (WAI 184)

TECHNICAL COMMITTEE: T-10 Concrete/ T-5 Loads

<input checked="" type="checkbox"/> REVISION	<input checked="" type="checkbox"/> ADDITION	<input type="checkbox"/> NEW DOCUMENT
<input checked="" type="checkbox"/> DESIGN SPEC	<input type="checkbox"/> CONSTRUCTION SPEC	<input type="checkbox"/> MOVABLE SPEC
<input checked="" type="checkbox"/> MANUAL FOR BRIDGE EVALUATION	<input type="checkbox"/> SEISMIC GUIDE SPEC <input type="checkbox"/> OTHER	<input type="checkbox"/> BRIDGE ELEMENT INSP GUIDE

DATE PREPARED: 9/10/14
DATE REVISED: 3/4/15

AGENDA ITEM:

Item #1

In Table 3.4.1-1, replace the load factor for live load in the Service III Load Combinations with γ_{LL} .

Item #2

In Article 3.4.1, add new Table 3.4.1-4 as follows:

Table 3.4.1-4—Load Factors for Live Load for Service III Load Combination, γ_{LL}

Component	γ_{LL}
<u>Prestressed concrete components designed using the refined estimates of time-dependent losses as specified in Article 5.9.5.4 in conjunction with taking advantage of the elastic gain</u>	<u>1.0</u>
<u>All other prestressed concrete components</u>	<u>0.8</u>

Item #3

In Article C3.4.1, revise the 10th paragraph and add the following paragraph:

Prior to 2014, the longitudinal analysis relating to tension in prestressed concrete superstructures was investigated using a load factor for live load of 0.8. The live load specified in these specifications This load factor reflects, among other things, current exclusion weight limits mandated by various jurisdictions at the time of the development of the specifications in 1993. Vehicles permitted under these limits have been in service for many years prior to 1993. It was concluded at that time that, for longitudinal loading, there is no nationwide physical evidence that these vehicles have caused cracking in existing prestressed concrete components. The 0.8 load factor was applied regardless of the method used for determining the loss of prestressing. The statistical significance of the 0.80 factor on live load is that the event is expected to occur about once a year for bridges with two traffic lanes, less often for bridges with a single traffic lane.

The calibration of the service limit states for concrete components (Wassef et al., 2014) concluded that typical components designed using the Refined Estimates of Time-Dependent Losses method incorporated in the specifications in 2005, which includes the use of transformed sections and elastic gains, have a lower reliability index against flexural cracking in prestressed components than components designed using the prestress loss calculation method specified prior to 2005 based on gross sections and do not include elastic gains. For components designed using the currently-specified methods for

instantaneous prestressing losses and the currently-specified Refined Estimates of Time-Dependent Losses method, an increase in the load factor for live load from 0.8 to 1.0 was required to maintain the level of reliability against cracking of prestressed concrete components inherent in the system.

Components which design satisfies all of the following conditions:

- The time-dependent prestressing losses are determined using either a refined time step method or the lump sum loss specified in Article 5.9.5.3
- The section properties are determined based on the concrete gross section, and
- The force in prestressing steel is determined without taking advantage of the elastic gain, were not affected by the changes in the prestressing loss calculation method introduced in 2005. For these components, a load factor for live load of 0.8 was maintained.

Service I should be used for checking tension related to transverse analysis of concrete segmental girders. The principal tensile stress check is introduced in order to verify the adequacy of webs of segmental concrete girder bridges for longitudinal shear and torsion.

Item #4

Add the following reference to Article 3.16:

Wassef, W. G., J. M. Kulicki, H. A. Nassif, A. S. Nowak and D. R. Mertz. 2014. *Calibration of LRFD Concrete Bridge Design Specifications for Serviceability*, Report on NCHRP 12-83 (in progress), Transportation Research Board, National Research Council, Washington, DC.

Item #5

In the Manual for Bridge Evaluation (MBE) Article 6A.4.2.2, revise Table 6A.4.2.2-1 as follows:

Table 6A.4.2.2-1—Limit States and Load Factors for Load Rating

Bridge Type	Limit State*	Dead Load γ_{DC}	Dead Load γ_{DW}	Design Load		Legal Load γ_{LL}	Permit Load γ_{LL}
				Inventory γ_{LL}	Operating γ_{LL}		
Steel	Strength I	1.25	1.50	1.75	1.35	Tables 6A.4.4.2.3a-1 and 6A.4.4.2.3b-1	—
	Strength II	1.25	1.50	—	—	—	Table 6A.4.5.4.2a-1
	Service II	1.00	1.00	1.30	1.00	1.30	1.00
	Fatigue	0.00	0.00	0.75	—	—	—
Reinforced Concrete	Strength I	1.25	1.50	1.75	1.35	Tables 6A.4.4.2.3a-1 and 6A.4.4.2.3b-1	—
	Strength II	1.25	1.50	—	—	—	Table 6A.4.5.4.2a-1
	Service I	1.00	1.00	—	—	—	1.00
Prestressed Concrete	Strength I	1.25	1.50	1.75	1.35	Tables 6A.4.4.2.3a-1 and 6A.4.4.2.3b-1	—
	Strength II	1.25	1.50	—	—	—	Table 6A.4.5.4.2a-1
	Service III	1.00	1.00	0.80 Table 6A.4.2.2-2	—	1.00	—
	Service I	1.00	1.00	—	—	—	1.00
Wood	Strength I	1.25	1.50	1.75	1.35	Tables 6A.4.4.2.3a-1 and 6A.4.4.2.3b-1	—
	Strength II	1.25	1.50	—	—	—	Table 6A.4.5.4.2a-1

In the MBE, add new Table 6A.4.2.2-2 as follows:

Table 6A.4.2.2-2—Load Factors for Live Load for the Service III Load Combination, γ_{LL} , at the Design-Load Inventory Level

Component	γ_{LL}
Prestressed concrete components rated using the refined estimates of time-dependent losses as specified in LRFD Design Article 5.9.5.4 in conjunction with taking advantage of the elastic gain	1.0
All other prestressed concrete components	0.8

In MBE Appendix B6A, revise Table B6A-1 as follows:

Table B6A-1—Limit States and Load Factors for Load Rating (6A.4.2.2-1)

Bridge Type	Limit State*	Dead Load γ_{DC}	Dead Load γ_{DW}	Design Load		Legal Load γ_{LL}	Permit Load γ_{LL}
				Inventory γ_{LL}	Operating γ_{LL}		
Steel	Strength I	1.25	1.50	1.75	1.35	Tables 6A.4.4.2.3a-1 and 6A.4.4.2.3b-1	—
	Strength II	1.25	1.50	—	—	—	Table 6A.4.5.4.2a-1
	Service II	1.00	1.00	1.30	1.00	1.30	1.00
	Fatigue	0.00	0.00	0.75	—	—	—
Reinforced Concrete	Strength I	1.25	1.50	1.75	1.35	Tables 6A.4.4.2.3a-1 and 6A.4.4.2.3b-1	—
	Strength II	1.25	1.50	—	—	—	Table 6A.4.5.4.2a-1
	Service I	1.00	1.00	—	—	—	1.00
Prestressed Concrete	Strength I	1.25	1.50	1.75	1.35	Tables 6A.4.4.2.3a-1 and 6A.4.4.2.3b-1	—
	Strength II	1.25	1.50	—	—	—	Table 6A.4.5.4.2a-1
	Service III	1.00	1.00	0.80 Table 6A.4.2.2-2	—	1.00	—
	Service I	1.00	1.00	—	—	—	1.00
Wood	Strength I	1.25	1.50	1.75	1.35	Tables 6A.4.4.2.3a-1 and 6A.4.4.2.3b-1	—
	Strength II	1.25	1.50	—	—	—	Table 6A.4.5.4.2a-1

In MBE Appendix B6A, add new Table B6A-2 as follows:

Table B6A-2—Load Factors for Live Load for the Service III Load Combination, γ_{LL} , at the Design-Load Inventory Level (6A.4.2.2-2)

Component	γ_{LL}
Prestressed concrete components rated using the refined estimates of time-dependent losses as specified in LRFD Design Article 5.9.5.4 in conjunction with taking advantage of the elastic gain	1.0
All other prestressed concrete components	0.8

Renumber the remaining tables in MBE Appendix B6A as follows:

Table B6A-2 becomes Table B6A-3

Table B6A-3 becomes Table B6A-4

Table B6A-4 becomes Table B6A-5

OTHER AFFECTED ARTICLES:

None

BACKGROUND:

A study of concrete service limit states reported in Wassef et al., 2014, found that there was a difference in reliability indices for prestressed concrete beams designed using loss calculations specified before and after 2005 which could be resolved with the proposed revisions.

ANTICIPATED EFFECT ON BRIDGES:

More consistent reliability when various loss methods are used.

REFERENCES:

Report on NCHRP 12-83 – in preparation
--

OTHER:

None

ATTACHMENT 2

Fatigue Agenda Item
From
the 2015 SCOBS Annual Meeting Agenda

2015 AASHTO BRIDGE COMMITTEE AGENDA ITEM: 3

SUBJECT: LRFD Bridge Design Specifications: Sections 3, 5 and 6, Various Articles

TECHNICAL COMMITTEE: T-5 Loads / T-10 Concrete / T-14 Steel

☒ **REVISION**
☒ **ADDITION**
☐ **NEW DOCUMENT**
☒ **DESIGN SPEC**
☐ **CONSTRUCTION SPEC**
☐ **MOVABLE SPEC**
☐ **MANUAL FOR BRIDGE EVALUATION**
☐ **SEISMIC GUIDE SPEC**
☐ **BRIDGE ELEMENT INSP GUIDE**
☐ **OTHER**

DATE PREPARED: 7/30/14

DATE REVISED: 3/5/15

AGENDA ITEM:

Item #1

Revise load factors for the Fatigue Limit States in Table 3.4.1-1 as follows:

Load Combination Limit State	DC DD DW EH EV ES EL PS CR SH	LL IM CE BR PL LS	WA	WS	WL	FR	TU	TG	SE	Use One of These at a Time				
										EQ	BL	IC	CT	CV
Strength I (unless noted)	γ_p	1.75	1.00	—	—	1.00	0.50/1.20	γ_{TG}	γ_{SE}	—	—	—	—	—
Strength II	γ_p	1.35	1.00	—	—	1.00	0.50/1.20	γ_{TG}	γ_{SE}	—	—	—	—	—
Strength III	γ_p	—	1.00	1.40	—	1.00	0.50/1.20	γ_{TG}	γ_{SE}	—	—	—	—	—
Strength IV	γ_p	—	1.00	—	—	1.00	0.50/1.20	—	—	—	—	—	—	—
Strength V	γ_p	1.35	1.00	0.40	1.0	1.00	0.50/1.20	γ_{TG}	γ_{SE}	—	—	—	—	—
Extreme Event I	γ_p	γ_{EQ}	1.00	—	—	1.00	—	—	—	1.00	—	—	—	—
Extreme Event II	γ_p	0.50	1.00	—	—	1.00	—	—	—	—	1.00	1.00	1.00	1.00
Service I	1.00	1.00	1.00	0.30	1.0	1.00	1.00/1.20	γ_{TG}	γ_{SE}	—	—	—	—	—
Service II	1.00	1.30	1.00	—	—	1.00	1.00/1.20	—	—	—	—	—	—	—
Service III	1.00	0.80	1.00	—	—	1.00	1.00/1.20	γ_{TG}	γ_{SE}	—	—	—	—	—
Service IV	1.00	—	1.00	0.70	—	1.00	1.00/1.20	—	1.0	—	—	—	—	—
Fatigue I— LL, IM & CE only	—	1.50 2.0	—	—	—	—	—	—	—	—	—	—	—	—
Fatigue II— LL, IM & CE only	—	0.75 0.80	—	—	—	—	—	—	—	—	—	—	—	—

Item #2

Revise the 3rd paragraph of Article C5.5.3.1 as follows:

In determining the need to investigate fatigue, Table 3.4.1-1 specifies a load factor of ~~1.50~~ on the live load force effect resulting from the fatigue truck for the Fatigue I load combination. This factored live load force effect represents the greatest fatigue stress that the bridge will experience during its life.

Item #3

Revise Eqs. 5.5.3.2-1 and 5.5.3.2-2 as follows:

$$\begin{aligned} \frac{(\Delta F)_{TH}}{f_y} &= 24 - 20 f_{\min} / f_y \\ (\Delta F)_{TH} &= 30 - 25 f_{\min} / f_y \end{aligned} \quad (5.5.3.2-1)$$

$$\begin{aligned} \frac{(\Delta F)_{TH}}{f_y} &= 16 - 0.33 f_{\min} / f_y \\ (\Delta F)_{TH} &= 20 - 0.41 f_{\min} \end{aligned} \quad (5.5.3.2-2)$$

Item #4

Add the following to the end of the second paragraph of Article C5.5.3.2:

Coefficients in Eqs. 5.5.3.2-1 and 5.5.3.2-2 have been updated based on calibration reported in Kulicki et al. (2014).

Item #5

Revise Table 6.6.1.2.3-2 as follows:

Table 6.6.1.2.3-2—75-yr $(ADTT)_{SL}$ Equivalent to Infinite Life

Detail Category	75-yrs $(ADTT)_{SL}$ Equivalent to Infinite Life (trucks per day)
A	530 <u>1030</u>
B	860 <u>1670</u>
B'	4035 <u>2015</u>
C	1290 <u>2510</u>
C'	745 <u>1455</u>
D	1875 <u>3660</u>
E	3530 <u>6890</u>
E'	6485 <u>12665</u>

Item #6

Revise Eq. C6.6.1.2.3-1 as shown:

$$\begin{aligned} \text{75-Year } (ADTT)_{SL} &= \frac{A}{\left[\frac{(\Delta F)_{TH}}{2} \right]^3 (365)(75)(n)} \\ \text{75-Year } (ADTT)_{SL} &= \frac{A}{\left[\frac{(\Delta F)_{TH}}{2.5} \right]^3 (365)(75)(n)} \end{aligned} \quad (C6.6.1.2.3-1)$$

Item #7

Revise Table 6.6.1.2.5-2 as follows:

Table 6.6.1.2.5-2—Cycles per Truck Passage, n

Longitudinal Members	Span Length	
	>40.0 ft	≤ 40.0 ft
Simple Span Girders	1.0	2.0
Continuous Girders		
1) near interior support	1.5	2.0
2) elsewhere	1.0	2.0
Cantilever Girders	5.0	
Orthotropic Deck Plate Connections Subjected to Wheel Load Cycling	5.0	
Trusses	1.0	
Transverse Members	Spacing	
	> 20.0 ft	≤ 20.0 ft
	1.0	2.0

Item #8

Add the following to the end of the first paragraph in Article C6.6.1.2.5:

Values of n for longitudinal members have been revised based on the calibration reported in Kulicki et al., 2014

Item #9

Add the following reference to Article 6.17:

Kulicki, J. M., W. G. Wassef, D. R. Mertz, A. S. Nowak, N. C. Samtani. 2014. Bridges for Service Life Beyond 100 Years: Service Limit State Design, Prepublication Draft. SHRP2, Transportation Research Board of the National Academies, Washington, DC.

OTHER AFFECTED ARTICLES:

None

BACKGROUND:

These proposed revisions are a product of the SHRP2 R19B project identified in Item #9. The revisions to the load factors for the Fatigue I and Fatigue II in Item #1 are a result utilizing WIM data to model live load as described below. The new load factors result directly in the changes shown in Items 1,4,5,6, and through calibration result in the changes in Item #3.

The use of the WIM data can be summarized below. Reference is made to “Probability Paper” throughout the summary. Normal probability paper is a special scale that facilitates the statistical interpretation of data. The horizontal axis represents the variable for which the cumulative distribution function (CDF) is plotted, e.g. gross vehicle weight (GVW), mid-span moment or shear. The vertical axis represents the number of standard deviations from the mean value. This is often referred to as the “Standard Normal Variable” or the “Z-Score.” The vertical axis can also be interpreted as probability of being exceeded and, for example, one standard deviation corresponds to 0.159 probability of being exceeded. The most important property of normal probability paper is that the CDF of a normal random variable is represented by a straight line. The straighter the plot of data, the more accurately it can be represented as a normal distribution. In addition, the curve representing the CDF of any other type of random variable can be evaluated and its shape can provide an indication about the statistical parameters such as the maximum value, type of distribution for the whole CDF or, if needed, only for the upper or lower tail of the CDF. Furthermore, the intersection of the CDF with horizontal axis (zero on vertical scale), corresponds to the mean. The slope of CDF determines the standard deviation, σ_x as shown below. A steeper CDF on probability paper indicates a smaller standard deviation.

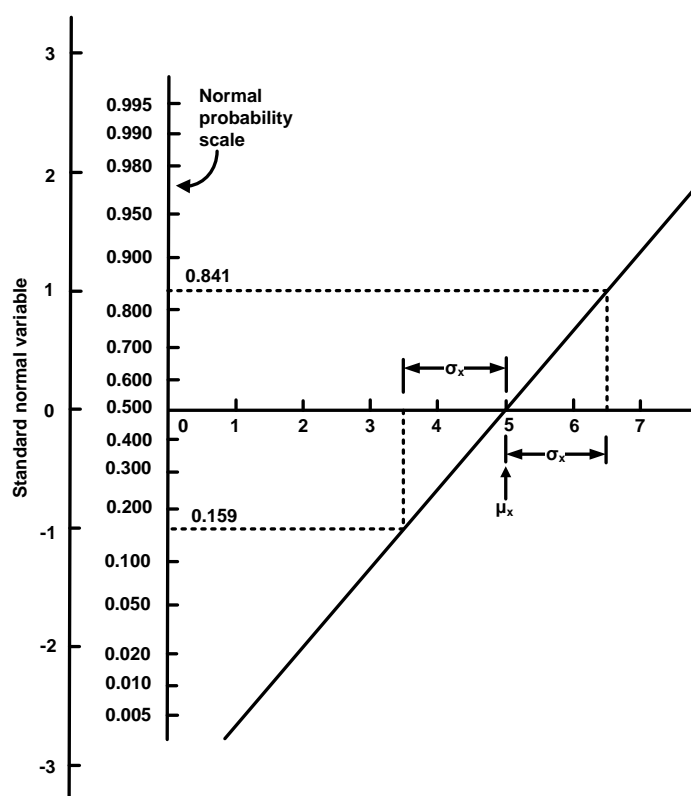


Figure 0-1 Use of normal probability paper.

Initially 65million data records were obtained from 31 sites. After filtering to eliminate records that seemed to be erroneous, elimination of a site for which the data we recorded in a unique format and other practical considerations about 35million records remained. For the purpose of the fatigue limit states, the 15 sites reported by the FHWA were selected for further processing.

Vehicles with GVW less than 20 kips were removed since they have been shown to add little to fatigue studies and add significantly to the work. This practical step has been used in previous studies.

For Fatigue II:

The complete string of vehicles for a given site was run across influence lines for simple spans (midspan) and two span continuous spans (moment at 0.4L and support) to produce a time history of moment for several span lengths.

The time history was then processed by commonly used rain-flow counting techniques to produce a series of events and the number of each event in the moment history. The number of events was divided by the number of trucks recorded at site to produce the average number of cycles per truck passage which led to the data in Item #7.

The string of events was then processed by the Pelgram-Miner process to produce the equivalent constant amplitude moment for each point considered for each span length considered. This was divided by the moment from the fatigue design truck specified in Article 3.6.1.4.1.

The resulting ratios were plotted on probability paper using a point from each of the 15 sites to produce a “curve” for each span for each of the moment location considered. The results were regular enough to be fitted with a straight line representing a normal distribution. The mean and bias of each line could then be read from the probability paper.

The biases were increased by 1.5 standard deviations and representative values were used to produce the load factor in Item #1 for Fatigue II, i.e. 0.80. The corresponding COV was 0.07.

For Fatigue I:

The rule of thumb that events greater than 1 in 10,000 may be ignored in the determination of the constant amplitude fatigue threshold was used in conjunction with the moments calculated from the WIM data by converting 0.0001 to a probability of not being exceeded of 0.9999 or 3.9 standard deviations past the mean value.

Using a horizontal line at 3.8 standard deviations to intercept the WIM data moments on probability paper for each span under consideration for each time of moment being considered resulted in a set of 15 point “curves” that could be reasonably well fitted with straight lines from which a mean and standard deviation could be determined.

Using the mean plus 1.5 standard deviations as the bias it was determined that a load factor of 2.0 was indicative of the results obtained: the COV was 0.12.

Calibration of Steel Details:

Reassessment of a set of fatigue test results assembled by Keating et.al. using a modified damage criteria developed for R19B and plotting the results on probability paper enabled the upper tail of the test results for each category to be fitted with a straight line defining the resistance for which the equation could be found.

Using the equations for resistance and other statistical data from the original LRFD calibration and the live load factors, Monte Carlo simulation were run to find the current and proposed reliability indices. It was found that the variability in reliability produced by the current provisions could be improved and the reliability of Fatigue I and II could be made almost equal by using the new load factor and either adding a set of resistance factors that ranged from 0.95 to 1.20 with reliability indices ranging from 0.90 to 1.20, or adjusting the S-N curves. The proposed changes to the resistance factors were small and applied primarily to the lesser used details. It was proposed to adjust the S-N curves. T-14 decided to support the changed load factors but decided that it was not advisable to change the S-N curves as many other specifications use the same curves.

Calibration of Reinforced Concrete:

Traditionally fatigue design of concrete and reinforcing elements is limited to Fatigue I, and prestressing elements are not designed for fatigue. These characteristics were retained in the R19B project.

Resistance data was taken from the literature. The data for reinforcing was reevaluated using the same

methods as described above for welded details.

The load factor and COV for live load was the same as for steel. Other data on uncertainties was taken from the original LRFD calibration.

Monte Carlo simulations resulted in current reliability indices of about 1.9 for reinforcing and 0.9 for concrete. The target reliability was set at 1.0 for steel elements and 0.9 for concrete which is generally consistent with that selected for other Service Limit States in the R19B project.

Recalibration to these reliability indices resulted in no change for concrete as it was determined that there was little sensitivity on the resistance side, and the proposed revisions for reinforcing and welded wire fabric.

ANTICIPATED EFFECT ON BRIDGES:

Some localized increase in fatigue demand.

REFERENCES:

SHRP2 R19B project report at <http://www.trb.org/Main/Blurbs/170201.aspx>

OTHER:

None

ATTACHMENT 3

Fatigue Agenda Item
From
the 2016 SCOBS Annual Meeting Agenda

2016 AASHTO BRIDGE COMMITTEE AGENDA ITEM: 11

SUBJECT: LRFD Bridge Design Specifications: Section 3, Article 3.4.1; Section 5, Article 5.5.3.2, and Section 6, Articles 6.6.1.2.3, 6.6.1.2.5 and 6.17

TECHNICAL COMMITTEE: T-14 Steel / T-5 Loads / T-10 Concrete

<input checked="" type="checkbox"/> REVISION	<input checked="" type="checkbox"/> ADDITION	<input type="checkbox"/> NEW DOCUMENT
<input checked="" type="checkbox"/> DESIGN SPEC	<input type="checkbox"/> CONSTRUCTION SPEC	<input type="checkbox"/> MOVABLE SPEC
<input type="checkbox"/> MANUAL FOR BRIDGE EVALUATION	<input type="checkbox"/> SEISMIC GUIDE SPEC	<input type="checkbox"/> BRIDGE ELEMENT INSP GUIDE
	<input type="checkbox"/> OTHER	

DATE PREPARED: 8/10/15

DATE REVISED:

AGENDA ITEM:

Item #1

In Column 3, revise Rows 12 and 13 of Table 3.4.1-1 as follows:

Fatigue I— LL, IM & CE only	—	1.50 1.75	—	—	—	—	—	—	—	—	—	—	—	—
Fatigue II— LL, IM & CE only	—	0.75 0.80	—	—	—	—	—	—	—	—	—	—	—	—

Item #2

Revise the last sentence of the 15th paragraph of Article C3.4.1 as follows:

In previous editions of these specifications, and in predecessor AASHTO bridge design specifications, the load factor for this load combination was chosen on the assumption that the maximum stress range in the random variable spectrum is twice the effective stress range caused by Fatigue II load combination. A reassessment of fatigue live load reported in Kulicki et al (2014) indicated that the load factors for Fatigue I and Fatigue II should be upgraded to the values now shown in Table 3.4.1-1 to reflect current truck traffic. The resulting ratio between the load factor for the two fatigue load combinations is 2.2.

Item #3

In Article 5.5.3.2, revise Eqs. 5.5.3.2-1 and 5.5.3.2-2 as follows:

$$(\Delta F)_{TH} = 24 - 20 f_{min} / f_y$$

$$(\Delta F)_{TH} = 26 - \frac{22 f_{min}}{f_y} \quad (5.5.3.2-1)$$

$$(\Delta F)_{TH} = 16 - 0.33 f_{min}$$

$$(\Delta F)_{TH} = 18 - 0.36 f_{min} \quad (5.5.3.2-2)$$

Item #4

In Article 6.6.1.2.3, revise Table 6.6.1.2.3-2 as follows:

Table 6.6.1.2.3-2—75-yr $(ADTT)_{SL}$ Equivalent to Infinite Life

Detail Category	75-yr $(ADTT)_{SL}$ Equivalent to Infinite Life (trucks per day)
A	530 <u>690</u>
B	860 <u>1120</u>
B'	1035 <u>1350</u>
C	1290 <u>1680</u>
C'	745 <u>975</u>
D	1875 <u>2450</u>
E	3530 <u>4615</u>
E'	6485 <u>8485</u>

Item #5

In Article C6.6.1.2.3, revise Eq. C6.6.1.2.3-1 as follows:

$$75_Year(ADTT)_{SL} = \frac{A}{\left[\frac{(\Delta F)_{TH}}{2} \right]^3 (365)(75)(n)}$$

$$75_Year(ADTT)_{SL} = \frac{A}{\left[\frac{0.80(\Delta F)_{TH}}{1.75} \right]^3 (365)(75)(n)} \quad (C6.6.1.2.3-1)$$

Item #6

In Article 6.6.1.2.5, revise Table 6.6.1.2.5-2 as follows:

Table 6.6.1.2.5-2—Cycles per Truck Passage, n

Longitudinal Members	Span Length	
	≥ 40.0 ft	≤ 40.0 ft
Simple Span Girders	1.0	2.0
Continuous Girders		
1) near interior support	1.5	2.0
2) elsewhere	1.0	2.0
Cantilever Girders	5.0	
Orthotropic	5.0	

Deck Plate Connections Subjected to Wheel Load Cycling		
Trusses	1.0	
Transverse Members	Spacing	
	>20.0 ft	≤20.0 ft
	1.0	2.0

Item #7

Add the following to the end of the 1st paragraph in Article C6.6.1.2.5:

Values of n for longitudinal members have been revised based on the calibration reported in Kulicki et al., 2014.

Item #8

Add the following reference to Article 6.17:

Kulicki, J. M., W. G. Wassef, D. R. Mertz, A. S. Nowak, and N. C. Samtani. 2014. Bridges for Service Life Beyond 100 Years: Service Limit State Design. Prepublication Draft. SHRP2, Transportation Research Board of the National Academies, Washington, DC.

OTHER AFFECTED ARTICLES:

None

BACKGROUND:

See Attachment A – Modified from the SHRP2 R19B Report

Item #3

The proposed revisions are an adaptation of the products of the SHRP2 R19B project identified in the references.

Fatigue design of concrete and reinforcing elements provides a theoretical finite life through the Fatigue I limit state load combination, and prestressing elements are not designed for fatigue. These characteristics were retained in the SHRP2 R19B project.

Fatigue resistance data was taken from the literature. The data for reinforcing was reevaluated using the same methods as for welded structural-steel details.

The load factor and COV for live load was the same as for steel. Other data on uncertainties was taken from the original LRFD calibration.

Monte Carlo simulations applying the existing fatigue provisions resulted in current reliability indices of about 2.0 for reinforcing and 1.0 for concrete. The target reliability was set at 1.0 for both steel elements and concrete which is generally consistent with that selected for other service limit states in the SHRP2 R19B project.

Recalibration to these reliability indices resulted in no change for concrete and the proposed revisions for reinforcing and welded wire fabric. The original work of SHRP2 R19B used a conservative live load distribution with the mean value assumed to be equal to the actual mean plus 1.5 standard deviations, if the data is considered limited. Technical committee work after the completion of the SHRP2 R19B project deemed the data abundant enough to use the actual mean instead of the mean plus 1.5 standard deviations. The constants and coefficient shown in Equations 5.5.3.2-1 and 5.5.3.2-2 are based upon this technical committee work and thus differ from those shown in the SHRP2 R19B final report.

ANTICIPATED EFFECT ON BRIDGES:

Some localized increase in fatigue demand. No effect. Fatigue does not control the design for typical reinforced-concrete structures.

REFERENCES:

SHRP2 R19B project report at <http://www.trb.org/Main/Blurbs/170201.aspx>

OTHER:

None

ATTACHMENT A (BACKGROUND) – 2015 AGENDA ITEM 11 - T-14 / T-5 / T-10

6.1 Fatigue Limit States – Lifetime

6.1.1 Steel Members

6.1.1.1 Formulate the Limit State Function

Two limit states for load-induced fatigue of steel details are defined in *AASHTO LRFD* Article 3.4.1: Fatigue I, related to infinite load-induced fatigue life; and Fatigue II, related to finite load-induced fatigue life.

For load-induced fatigue considerations, according to *AASHTO LRFD* Article 6.6.1.2.2, each steel detail shall satisfy:

$$\gamma(\Delta f) \leq (\Delta F)_n \quad (6.1.1.1-1)$$

where:

- γ = load factor
- (Δf) = force effect, live load stress range due to the passage of the fatigue load
- $(\Delta F)_n$ = nominal fatigue resistance

This general limit state function is used for the calibration of the fatigue limit states.

The fatigue load of *AASHTO LRFD* Article 3.7.1.4 and the fatigue live load load factors of *AASHTO LRFD* Table 3.4.1-1 are based upon extensive research of structural-steel highway bridges. The fatigue load is the *AASHTO LRFD* design truck (HS20-44 truck of *AASHTO Standard Specifications*, 2002), but with a fixed rear-axle spacing of 30 feet. The live load load factors for the fatigue limit state load combinations are summarized in Table 6.1.1.1-1.

Table 6.1.1.1-1 Current Fatigue Load Factors

Fatigue Limit state	LL Load Factor
Fatigue I	1.5
Fatigue II	0.75

The load factor for the Fatigue I load combination reflects load levels found to be representative of the maximum stress range of the truck population for infinite fatigue-life design. The factor was chosen on the assumption that the maximum stress range in the random variable spectrum is twice the effective stress range caused by Fatigue II load combination.

The load factor for the Fatigue II load combination reflects a load level found to be representative of the effective stress range of the truck population with respect to a small number of stress range cycles and to their cumulative effects in steel elements, components, and connections for finite fatigue-life design.

The resistance factors for the fatigue limit states, ϕ , are inherently taken as unity and hence do not appear in Eq. 6.1.1.1-1

6.1.1.2 Select Structural Types and Design Cases

Components and details susceptible to load-induced fatigue cracking have been grouped into eight groups, called detail categories, by fatigue resistance. *AASHTO LRFD* Table 6.6.1.2.3-1 illustrates many common details found in steel bridge construction and identifies potential crack sites for each detail. Figure 6.1.1.2-1 shows the current *AASHTO LRFD* fatigue design curves with the detail categories ranging from A to E'.

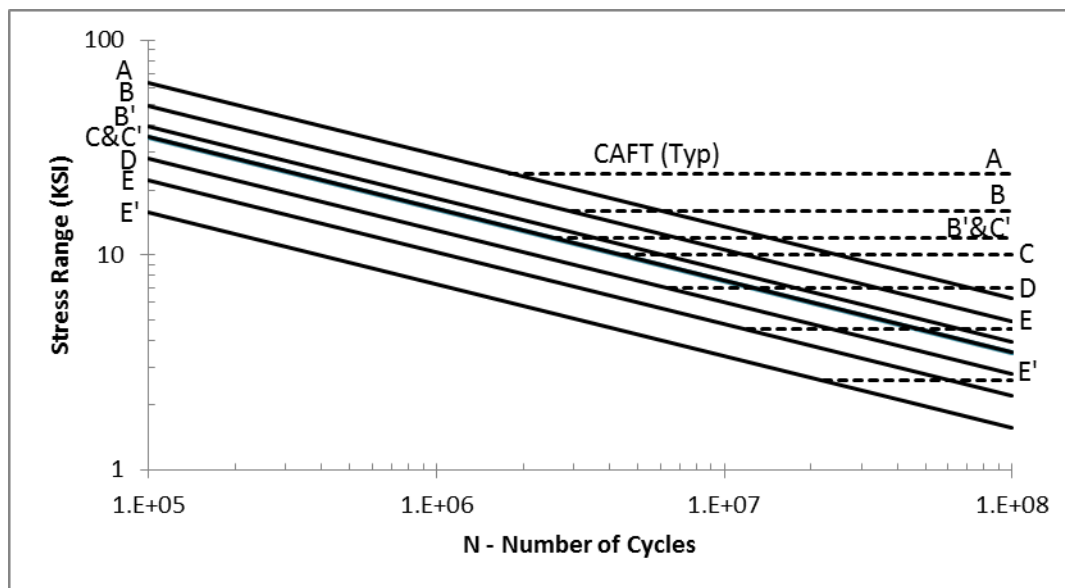


Figure 6.1.1.2-1 AASHTO fatigue design curves: stress range versus number of cycles (AASHTO 2012). (Used with permission of the American Association of State Highway and Transportation Officials)

6.1.1.3 Determine Load and Resistance Parameters for Selected Design Cases

A comprehensive database containing constant and variable amplitude fatigue test results for various welded steel bridge detail types was developed by Keating and Fisher (1986). This database includes the test data from the various NCHRP test programs and other available data as indicated in the database.

The fatigue data includes the detail type of each specimen, the minimum and maximum stress values, as well as the number of cycles observed until fatigue failure was evident. From this data, the stress range is taken as the only significant parameter in the determination of the fatigue life, thus a relationship between the stress range and number of cycles to failure was developed for the combined fatigue data (Keating and Fisher, 1986). The regression analysis performed on the stress range versus cycle relation showed that this relation was log-log in nature. The curves of the data plotted in log form are characterized by:

$$\log N = \log A - B \log S_r \quad (6.1.1.3-1)$$

or in exponential form:

$$N = A S_r^{-B} \quad (6.1.1.3-2)$$

where:

- N = number of cycles to failure
 S_r = constant amplitude stress range, ksi
 $\log A$ = log-N-axis intercept of S-N curve, a constant taken from *AASHTO LRFD* Table 6.6.1.2.5-1 for the various detail categories
 B = slope of the curve

The combined fatigue data for each detail type was categorized into the eight different detail categories based on the fatigue performance of the details as specified by *AASHTO LRFD* Article 6.6.1.2.3. Fatigue design curves were then determined for each of the fatigue categories. The design curves represent allowable stress range values that are based on a 98 percent confidence limit, or lower bound of fatigue resistance. Thus, for a particular detail type, most of the fatigue data falls above the design curve and the test data should not deviate significantly from the curve. The slope of the all of the design curves were determined to be very close to a constant value of -3.0 as shown through the use of regression analysis (Keating and Fisher, 1986). Thus, a constant slope of -3.0 was imposed on the equations in the regression analysis. Figure 6.1.1.2-1 shows the current *AASHTO LRFD* fatigue design curves with the detail categories ranging from A to E'.

6.1.1.4 Develop Statistical Models for Loads and Resistances

6.1.1.4.1 Load Uncertainties

Based on the analysis of WIM data discussed in Chapter 5 of the SHRP2 R19B report, it is suggested that the current load factor of 1.5 for the Fatigue I limit state be increased to 1.75 to account for current and projected truck loads. Similarly, it is proposed that the load factor of 0.75 for the Fatigue II limit state be increased to a value of 0.80. The mean values and COVs from Chapter 5 are tabulated below.

Table 6.1.1.4.1-1 Load Uncertainties

Limit State	Mean	COV
Fatigue I	1.75	0.12
Fatigue II	0.8	0.07

6.1.1.4.2 Resistance Uncertainties

6.1.1.4.2a Fatigue Damage Parameter

In order to properly calibrate the fatigue limit states of the *AASHTO LRFD*, it is necessary to determine the statistical parameters of the fatigue test data used in the bridge fatigue resistance model. These parameters include the bias and the COV of the fatigue test data. As previously described the fatigue data is commonly presented in terms of the stress range and number of cycles to failure, or S-N curves in log-log space. The use of this relationship with the given constant amplitude fatigue test data, however, causes difficulty in accurately determining the statistical parameters. The available data was not sufficiently distributed along the S-N curves in log-log space for a regression analysis as the data was often gathered over a small increment of stress ranges and was limited in number. Any number of regression lines could have been used to describe this relationship between the stress range and fatigue life. Thus in order to better analyze the fatigue data a different relationship between the number of cycles and stress range was developed.

The test data was arranged to couple the number of cycles and stress range together in the form of an effective stress range for each test specimen. The effective stress range as presented in Article 6.6.2.2 of *AASHTO LRFD* (2010) is taken as the cube root of the sum of the cubes of the measured stress ranges as

seen in Eq. 6.1.1.4.2a-1 below. The effective stress range is an accepted means to compare variable-amplitude fatigue data to constant-amplitude fatigue test data.

$$(S_r)_{\text{eff}} = \left(\sum \gamma_i S_{ri}^3 \right)^{1/3} \quad (6.1.1.4.2a-1)$$

where:

$$\begin{aligned} (S_r)_{\text{eff}} &= \text{effective constant amplitude stress range} \\ \gamma_i &= \text{percentage of cycles at a particular stress range} \\ S_{ri} &= \text{constant amplitude stress range for a group of cycles (ksi)} \end{aligned}$$

The formula describing the parameter used for the test data follows the form of the above equation; however, this equation is applied to each of the test specimens. Thus the percentage term is equated to a value of one and is subsequently multiplied by the number of cycles, N, to yield the following equation:

$$S_{fi} = \left(N * S_{ri}^3 \right)^{1/3} \quad (6.1.1.4.2a-2)$$

where:

$$S_{fi} = \text{fatigue damage parameter}$$

This fatigue parameter is taken as a normally distributed random variable in order to determine the bias and coefficient of variation of the fatigue resistance for each of the detail categories. The data was fitted to many of the typical distributions commonly used and it was determined that the normal distribution best characterized the nature of the fatigue data. The bias is a ratio of the mean value of the test data to the nominal value described in the specifications. The calculation of the nominal, mean, and coefficient of variation values are described in the subsequent sections.

6.1.1.4.2b Probability Paper to Determine Statistical Parameters

The collection of the fatigue data in terms of the new fatigue parameter for each detail category was then statistically analyzed using normal probability paper as the data best fits the normal distribution. The fatigue data for each detail category was then filtered to include the data that most accurately reflects the fatigue behavior of each category. In other words, the data was truncated based on the nature of the curve within each normal probability plot to include the pertinent fatigue data. In general, the majority of the lower portion of each curve was selected for each detail category. The lower tail of the data was selected because it is the portion of the curve that fits the normal distribution, as it is the straight portion of the normal probability plot. Moreover, the lower portion of the fatigue data represents the range of values within which fatigue cracking is expected to occur when analyzed for the fatigue limit state load combinations using the Monte Carlo simulation approach which is discussed in more detail later. Failure occurs when the load exceeds the resistance; thus the higher portions of the fatigue data sets represent fatigue resistance data that are very unlikely to be exceeded by the fatigue loads used within this study and therefore are insignificant.

Different approaches for selecting the cutoff values for each category were investigated to determine the sensitivity of the resulting reliability indices. It was determined that the relative difference of the results determined from the different techniques were negligible. Other techniques used to determine the cutoff values included the use of constant cutoff values for all of the various detail categories as well as manually inserting best-fit lines by different analysts. Table 6.1.1.4.2c-1 shows the resulting cutoff values

for the standard normal variable. Figure 6.1.1.4.2b-1 and Figure 6.1.1.4.2b-2 show the normal probability plots of the full fatigue data set and the truncated data for categories C and C' respectively.

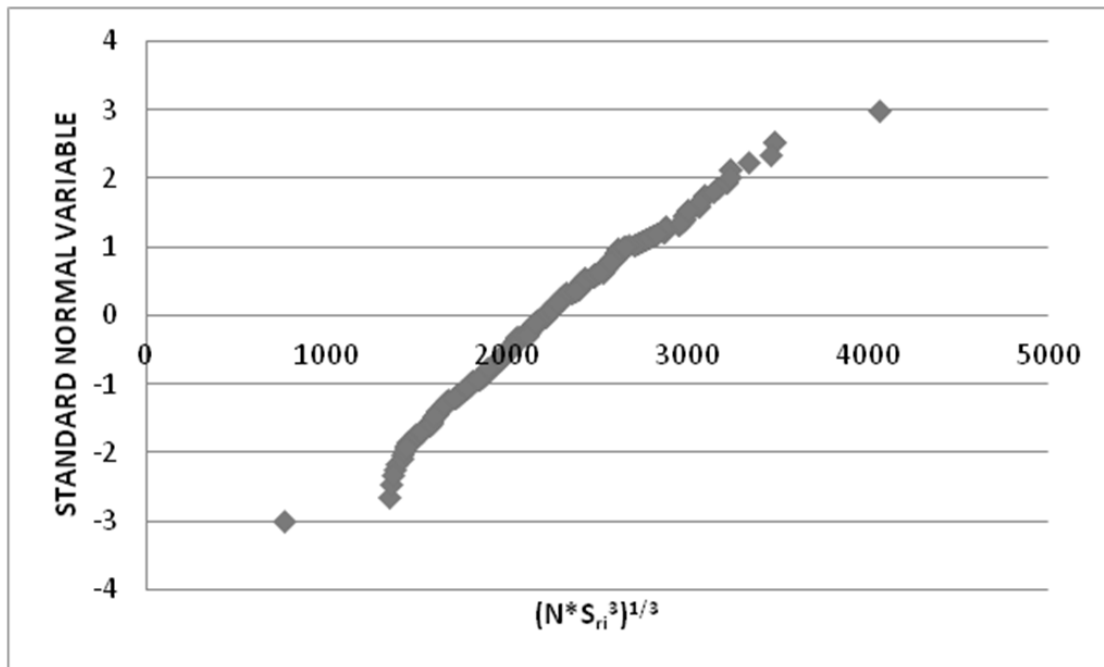


Figure 6.1.1.4.2b-1 Normal probability plot of detail categories C and C' fatigue data.

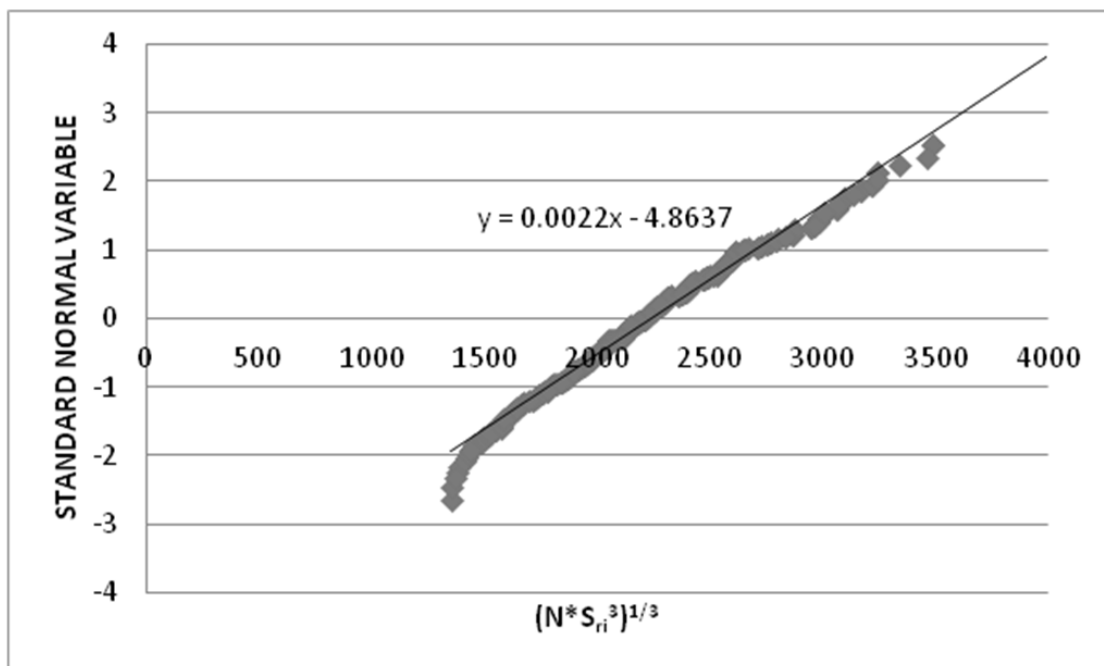


Figure 6.1.1.4.2b-2 Normal probability plot of detail categories C and C' truncated fatigue data with best fit line.

Determining the statistical parameters of the data is relatively straightforward once the data for each detail category was filtered and fitted with a line of best fit using Microsoft Excel software. The mean value of the stress parameter is simply the intersection of the best fit line with the horizontal axis. The standard deviation of the data is taken as the inverse of the slope of the best fit line. More simply stated it is the change in horizontal coordinates divided by the change in the vertical coordinates. Moreover, the coefficient of variation is the ratio of the standard deviation to the mean of the data. The resulting statistical parameters are given in Table 6.1.1.2.4c-1. The probability plots of the fatigue data and corresponding truncated data for all detail categories can be seen in Appendix E.

6.1.1.4.2c Determination of Nominal Fatigue Parameter and Bias Values

The coefficient of variation and the mean of the fatigue resistance data was determined as described in the previous section. These values along with the nominal fatigue resistance are needed to determine the bias of the data. The nominal value of the chosen fatigue parameter was calculated using *AASHTO LRFD* Eq. 6.6.1.2.5-2 and rearranged to achieve the relationship in terms of the desired fatigue damage parameter, as seen in the following equation. The resulting nominal resistance values can be seen in Table 6.1.1.4.2c-1.

$$S_{f-AASHTO} = (N * S_r^3)^{1/3} = A^{1/3} \quad (6.1.1.4.2c-1)$$

where:

$S_{f-AASHTO}$ = nominal value of the fatigue parameter using *AASHTO LRFD Specifications* for each detail category

A = constant taken from *AASHTO LRFD* Table 6.6.1.2.5-1 for the various detail categories

The bias value for each category is determined by simply taking the ratio of the mean value to the nominal value of the fatigue parameter as seen in the following equation; the results are shown in Table 6.1.1.4.2c-1.

$$Bias = S_{f_Mean} / S_{f_AASHTO} \quad (6.1.1.4.2c-2)$$

where:

S_{f_Mean} = mean value of the fatigue parameter using the fatigue data for each detail category

Table 6.1.1.4.2c-1 Resistance Uncertainties

Category	Standard Deviation	COV	Bias	S_{f_Mean}	S_{f_AASHTO}	Cutoff Standard Normal Variable
A	1000.0	0.24	1.43	4167.40	2924	1
B	666.7	0.22	1.34	3077.47	2289	1
B'	250.0	0.11	1.28	2336.10	1827	1
C and C'	454.6	0.21	1.35	2210.77	1638	1
D	185.2	0.10	1.36	1773.69	1300	1
E	140.9	0.12	1.17	1207.41	1032	1
E'	232.6	0.20	1.56	1140.28	730	1

6.1.1.5 Develop the Reliability Analysis Procedure

6.1.1.5.1 General

In code calibration, it is necessary to develop a process by which to express the structural reliability or the probability of the loads on the member being greater than its resistance; in other words, failure of the criteria. The reliability analysis performed within this project is an iterative process that consists of Monte Carlo simulations to select load and resistance factors that achieve reliability close to the target reliability index. The Monte Carlo technique samples load and resistance parameters from selected statistical distributions, such as a normal distribution. The reliability is measured in terms of a reliability index, or safety index, β . β is defined as a function of the probability of failure, PF , using the following equation. Thus β is the number of standard deviations that the mean safety margin falls on the safe side. The higher the β value, the higher the reliability.

$$\beta = -\Phi^{-1}(PF) \quad (6.1.1.5.1-1)$$

where:

Φ^{-1} = the inverse standard normal distribution function

6.1.1.5.2 Monte Carlo Simulation

The Monte Carlo Analysis is described more fully in Section 3.2.3 of the SHRP2 R19B report. A step-by-step outline of the Monte Carlo simulation using Microsoft Excel is included in Appendix F of that report.

The distribution of loads is assumed to be normally distributed as the loads are a summation of force effects. The fatigue resistance has also been assumed to follow normal distributions. These distributions for load and resistance are developed using determined statistical parameters from the available data.

6.1.1.6 Calculate the Reliability Indices for Current Design Code or Current Practice

The current reliability indices inherent for the various fatigue detail categories were determined using the aforementioned Monte Carlo simulation technique with the provisions for the Fatigue I and II limit states as specified in the *AASHTO LRFD*. The Fatigue I limit state utilizes a load factor of 1.5 which is common to all of the detail types. The coefficient of variation for the Fatigue I limit state was determined to be 0.12 through the work discussed in Section 5. The resistance parameters for the Monte Carlo simulation were then determined by equating the nominal load and resistance values and then applying the statistical parameters for each of the detail categories which can be found in Table 6.1.1.4.2c-1. Insufficient fatigue data exists for the constant amplitude fatigue threshold (CAFT) portions of the fatigue design curves for the finite fatigue design life (Fatigue II limit state). In consultation with AASHTO Technical Committee T-14 and the AISI BTF, was deemed acceptable to use the statistical parameters for the sloping portions of these curves for the constant amplitude fatigue thresholds of the different bridge detail categories. In *AASHTO LRFD*, the Fatigue II limit state currently has a load factor of 0.75 for all of the detail categories and a coefficient of variation of 0.07. The nominal resistance values were determined using the following equation which results from setting the *AASHTO LRFD* fatigue resistance Eq. 6.6.1.2.5-2 equal to the design fatigue load which is normalized to a stress range equal to 1 ksi.

$$R = A / 0.75^3 \quad (6.1.1.6-1)$$

where:

R = resistance

A = constant taken from *AASHTO LRFD* Table 6.6.1.2.5-1 for the various detail categories

The simulations for both limit states were completed using a total of 10,000 replicates to achieve a sufficient number of failures. The resulting current reliability indices for each of the eight detail categories are reported in Table 6.1.1.6-1.

Table 6.1.1.6-1 Current Reliability Indices Using *AASHTO LRFD* Fatigue I and Fatigue II Limit States

Category	β	
	Fatigue I	Fatigue II
A	1.2	1.0
B	1.1	0.9
B'	1.5	1.0
C	1.2	0.9
C'	1.2	0.9
D	2.0	1.3
E	0.9	0.7
E'	1.7	1.4

6.1.1.7 Select the Target Reliability Index, β_T

Target reliability indices are based upon the inherent reliability of the current specifications, shown in Table 6.1.1.6-1. The fatigue limit states are harmonized by selecting a single, common target reliability index for both steel and concrete members equal to 1.0. This proposed target was selected to best reflect the inherent reliability of the Fatigue I and II limit states for structural steel members and Fatigue I limit state for reinforcement and concrete.

6.1.1.8 Select Potential Load and Resistance Factors

When the proposed load factors of 1.75 and 0.8, for the Fatigue I and Fatigue II limit states respectively, and the inherent resistance factor of 1.0 is applied along with the statistical data, the reliability indices for each detail category remain essentially unchanged from those reported in Table 6.1.1.6-1. Accepting a range of ± 0.2 on the reliability index, three Fatigue I limit state reliability indices appear to be too large: detail category B' at $\beta=1.5$, detail category D at $\beta=2.0$ and detail category E' at $\beta=1.7$. Similarly, two Fatigue II limit state reliability indices appear to be too large, detail category D at $\beta=1.3$ and detail category E' at $\beta=1.4$; and one appears to be too small, detail category E at $\beta=0.7$.

Proposed resistance factors for the Fatigue I limit state and the Fatigue II limit state are given in Table 6.1.1.8-1 and Table 6.1.1.8-2, respectively. Resistance factors other than the current values of unity are shown in boldface. Reliability index values using the proposed resistance factors are shown in the last column.

Table 6.1.1.8-1 Proposed Fatigue I Limit State Resistance Factors

Detail Category	Proposed Resistance Factor, ϕ	Reliability Index, β
A	1.0	1.2
B	1.0	1.1
B'	1.10	0.9
C	1.0	1.2
C'	1.0	1.2
D	1.15	1.1
E	1.0	0.9
E'	1.20	1.0

Table 6.1.1.8-2 Proposed Fatigue II Limit State Resistance Factors

Detail Category	Proposed Resistance Factor, ϕ	Reliability Index, β
A	1.0	1.0
B	1.0	0.9
B'	1.0	1.0
C	1.0	0.9
C'	1.0	0.9
D	0.95	1.0
E	1.10	1.0
E'	0.90	1.0

With the proposed resistance factors, the reliability indices are all within ± 0.2 of the target reliability index of 1.0. It was eventually decided during the specification adoption process to keep the resistance factors equal at 1.0 for all categories.

ATTACHMENT 4

Service I, Deflection, Agenda Item
From
the 2015 SCOBS Annual Meeting Agenda

2015 AASHTO BRIDGE COMMITTEE AGENDA ITEM: 11

SUBJECT: LRFD Bridge Design Specifications: Section 2, Articles 2.5.2.6.2 and 2.8

TECHNICAL COMMITTEE: T-14 Steel / T-5 Loads

<input checked="" type="checkbox"/> REVISION	<input checked="" type="checkbox"/> ADDITION	<input type="checkbox"/> NEW DOCUMENT
<input checked="" type="checkbox"/> DESIGN SPEC	<input type="checkbox"/> CONSTRUCTION SPEC	<input type="checkbox"/> MOVABLE SPEC
<input type="checkbox"/> MANUAL FOR BRIDGE EVALUATION	<input type="checkbox"/> SEISMIC GUIDE SPEC	<input type="checkbox"/> BRIDGE ELEMENT INSP GUIDE
	<input type="checkbox"/> OTHER	

DATE PREPARED: 7/30/14

DATE REVISED: 9/30/14

AGENDA ITEM:

Item #1

In Article 2.5.2.6.2, revise the 3rd bullet after the 3rd paragraph as follows:

- For composite design, the stiffness of the design cross-section used for the determination of deflection and frequency should include the entire width of the roadway and the structurally continuous portions of the railings, sidewalks, and median barriers;

Item #2

Add the following to Article C2.5.2.6.2 opposite the 4th paragraph of specification:

Other criteria may include recognized deflection-frequency-perception requirements such as that specified in the *Canadian Highway Bridge Design Code* (CSA, 2006). Application of the CSA criteria is discussed in Kulicki et. al., (2014), including statistical data for live load based on WIM data, a load factor for the HL-93 live load and a target reliability index.

Item #3

Add the following references to Article 2.8:

CSA. 2006. *Canadian Highway Bridge Design Code*. CAN/CSA-S6-06. Includes Supplement 1, Supplement 2, and Supplement 3. Canadian Standards Association International, Toronto, ON, Canada.

Kulicki, J. M., W. G. Wassef, D. R. Mertz, A. S. Nowak, and N. C. Samtani. 2014. *Bridges for Service Life Beyond 100 Years: Service Limit State Design*, Prepublication Draft. SHRP2, Transportation Research Board of the National Academies, Washington, DC.

OTHER AFFECTED ARTICLES:

None

BACKGROUND:

This commentary revision is a product of SHRP2 R19B, Bridges for Service Life Beyond 100 Years: Service Limit State Design which focused on calibration of Service Limit States in AASHTO LRFD similar to the calibration of the Strength Limit State during the original development of AASHTO LRFD. In the case of this limit state often referred to as deflection control there was found to be limited accepted criteria on dynamic response to live load. The frequency-deflection-perception criteria currently in the CSA Canadian Bridge Design Code (previously in the OHBDC) was chosen as it accounts for more of the basic parameters than the current AASHTO span/constant criteria. Never-the-less, a comparison using 41 sample bridges from the NCHRP 12-78 database indicated a trend-wise similarity as indicated in the figures below taken from the R19B report.

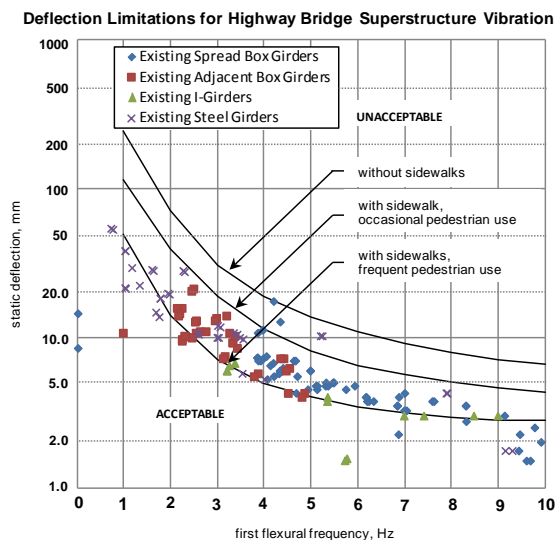


Figure 0-1 Comparison of CHBDC requirement and various bridges satisfying all AASHTO design requirements

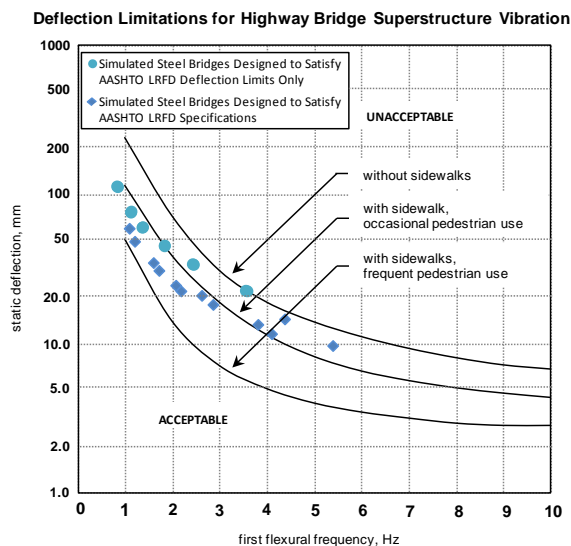


Figure 0-2 Comparison of CHBDC requirements and various steel bridges satisfying all AASHTO design requirements and similar bridges satisfying only L/800

A calibration based on the statistics of live load found in the R19B study of WIM data from 31 sites (Bias of 1.35 and COV of 0.12 compared to HL93, annual return, ADTT 5000, CHBDC curves considered deterministic) indicated that a load factor of 1.50 would be required.

A limited study on material requirements using either the current requirements and those in Attachment A for steel

simple span bridges indicated that impacts were small and limited to very short bridges.

Based on the above discussion and other details in the R19B report, the following summary regarding this limit state was made:

“Based on this research there does not appear to be a compelling need to change the current AASHTO LRFD provision for live load response, i.e. load deflection in Article 2.5.6.2. Such an approach is basically “deemed to satisfy.” However, if AASHTO chooses to adopt the more complete approach of combining frequency, displacement, and perception a possible set of revisions to accomplish that change are proposed”

T-14 recommended a minor change to the specification with the addition of further commentary. T-5 agrees with the change to the Specification and a shortened version of the additional commentary as indicated.

ANTICIPATED EFFECT ON BRIDGES:

Structure Dependent

REFERENCES:

See Background

OTHER:

None

ATTACHMENT 5

Proposed 2016 Meeting Foundations Deformations Agenda Item
(as of November 2016)

Proposed Modifications to Section 3

TABLE OF CONTENTS

[illegible]

-
-
-
-

3.3—NOTATION

3.3.1—General

A = plan area of ice floe (ft²); depth of temperature gradient (in.) (C3.9.2.3) (3.12.3)

~~A_d = factored angular distortion (rad) (Appendix C3)~~

AEP = apparent earth pressure for anchored walls (ksf) (3.4.1)

-
-

L = perimeter of pier (ft); length of soil reinforcing elements in an MSE wall (ft); length of footing (ft); expansion length (in.) (3.9.5) (3.11.5.8) (3.11.6.3) (3.12.2.3)

~~L_s = span length (ft) (Appendix C3)~~

$LLDF$ = live load distribution factor as specified in Table 3.6.1.2.6-1a (3.6.1.2.6b)

-
-

r = radius of pier nose (ft) (C3.9.2.3)

~~S = Settlement (ft) (Appendix C3)~~

S_{DS} = horizontal response spectral acceleration coefficient at 0.2-s period modified by short-period site factor (3.10.4.2)

-
-

δ = angle of truncated ice wedge (degrees); friction angle between fill and wall (degrees); angle between the far and near corners of a footing measured from the point on the wall under consideration (rad) ~~foundation deformation (rad. or in.) (C3.9.5) (3.11.5.3) (3.11.6.2) (Appendix C3)~~

~~δ_e = factored deformation (rad. or in.) (Appendix C3)~~

η_i = load modifier specified in Article 1.3.2; wall face batter (3.4.1) (3.11.5.9)

-
-
-
-
-

3.4—LOAD FACTORS AND COMBINATIONS

3.4.1—Load Factors and Load Combinations

The total factored force effect shall be taken as:

$$Q = \sum \eta_i \gamma_i Q_i \tag{3.4.1-1}$$

- η_i = load modifier specified in Article 1.3.2
- Q_i = force effects from loads specified herein
- γ_i = load factors specified in Tables 3.4.1-1 and ~~to~~ 3.4.1-52

-
-
-
-
-

The evaluation of overall stability of retained fills, as well as earth slopes with or without a shallow or deep foundation unit should be investigated at the service limit state based on the Service I Load Combination and an appropriate resistance factor as specified in Article 11.5.6 and Article 11.6.2.3.

The investigation of foundation settlement shall proceed using the provisions of Article 10.6.2.4 using the load factor, γ_{SF} , specified in Table 3.4.1-4 3.4.1-5.

For structural plate box structures complying with the provisions of Article 12.9, the live load factor for the vehicular live loads *LL* and *IM* shall be taken as 2.0.

The load factor for temperature gradient, γ_{TG} , should be considered on a project-specific basis. In lieu of project-specific information to the contrary, γ_{TG} may be taken as:

C3.4.1

The background for the load factors specified herein, and the resistance factors specified in other Sections of these Specifications is developed in Nowak (1992).

Applying these criteria for the evaluation of the sliding resistance of walls:

- The vertical earth load on the rear of a cantilevered retaining wall would be multiplied by γ_{pmin} (1.00) and the weight of the structure would be multiplied by γ_{pmin} (0.90) because these forces result in an increase in the contact stress (and shear strength) at the base of the wall and foundation.
- The horizontal earth load on a cantilevered retaining wall would be multiplied by γ_{pmax} (1.50) for an active earth pressure distribution because the force results in a more critical sliding force at the base of the wall.

Similarly, the values of γ_{pmax} for structure weight (1.25), vertical earth load (1.35) and horizontal active earth pressure (1.50) would represent the critical load combination for an evaluation of foundation bearing resistance.

Water load and friction are included in all strength load combinations at their respective nominal values.

For creep and shrinkage, the specified nominal values should be used. For friction, settlement, and water loads, both minimum and maximum values need to be investigated to produce extreme load combinations.

The load factor for temperature gradient should be determined on the basis of the:

- Type of structure, and

- 0.0 at the strength and extreme event limit states,
- 1.0 at the service limit state when live load is not considered, and
- 0.50 at the service limit state when live load is considered.

The effects of the foundation deformation on the bridge superstructure, retaining walls, or other load bearing structures shall be evaluated at applicable strength and service limit states using the provisions of Article 10.5.2.2 and the settlement load factor (γ_{SE}) specified in Table 3.4.1-4. For all bridges, stiffness should be appropriate to the considered limit state. Similarly, the effects of continuity with the substructure should be considered. In assessing the structural implications of foundation deformations of concrete bridges, the determination of the stiffness of the bridge components should consider the effects of cracking, creep, and other inelastic responses.

The load factor for settlement, γ_{SE} , should be considered on a project specific basis [NCS1]. In lieu of project specific information to the contrary, γ_{SE} may be taken as 1.0. Load combinations which include settlement shall also be applied without settlement. As specified in Article 3.12.6, differential settlement between and within substructure units shall be considered when determining extreme combinations of force effects.

For segmentally constructed bridges, the following combination shall be investigated at the service limit state:

$$DC + DW + EH + EV + ES + WA + CR + SH + TG + EL + PS$$

(3.4.1-2)

- Limit state being investigated.

Open girder construction and multiple steel box girders have traditionally, but perhaps not necessarily correctly, been designed without consideration of temperature gradient, i.e., $\gamma_{TG} = 0.0$.

The values of γ_{SE} in Table 3.4.1-5 are based on a target reliability index, β , of 0.50 which assumes that the effect of irreversible foundation deformations on the bridge superstructure will be reversed by intervention, e.g., shimming, jacking, etc. If intervention to relieve the superstructure is not practical or desirable for a given bridge type, then larger values of γ_{SE} consistent with target reliability index of 1.00 or larger shall be considered based on Kulicki et al., (2015) and Samtani and Kulicki (2016).

An owner may choose to use a local method that provides better estimation of foundation movement for local geologic conditions compared to methods noted in Section 10. In such cases, the owner will have to calibrate the γ_{SE} value for the local method using the procedures described in Kulicki et al., (2015) and Samtani and Kulicki (2016).

The value of $\gamma_{SE} = 1.00$ for consolidation (long-term settlement time-dependent) settlement assumes that the estimation of consolidation settlement is based on appropriate laboratory and field tests to determine parameters (rather than correlations with index properties of soils) in the consolidation settlement equations in Article 10.6.2.4.3.

The value of γ_{SE} should be calibrated using procedures described in Kulicki et al., (2015) and Samtani and Kulicki (2016).

[illegible]

Table 3.4.1-2—Load Factors for Permanent Loads, γ_p

Type of Load, Foundation Type, and Method Used to Calculate Downdrag		Load Factor	
		Maximum	Minimum
<i>DC</i> : Component and Attachments		1.25	0.90
<i>DC</i> : Strength IV only		1.50	0.90
<i>DD</i> : Downdrag	Piles, α Tomlinson Method	1.4	0.25
	Piles, λ Method	1.05	0.30
	Drilled shafts, O’Neill and Reese (1999) Method	1.25	0.35
<i>DW</i> : Wearing Surfaces and Utilities		1.50	0.65
<i>EH</i> : Horizontal Earth Pressure			
Active		1.50	0.90
At-Rest		1.35	0.90
<i>AEP</i> for anchored walls		1.35	N/A
<i>EL</i> : Locked-in Construction Stresses		1.00	1.00
<i>EV</i> : Vertical Earth Pressure			
Overall Stability		1.00	N/A
Retaining Walls and Abutments		1.35	1.00
Rigid Buried Structure		1.30	0.90
Rigid Frames		1.35	0.90
Flexible Buried Structures			
o Metal Box Culverts, Structural Plate Culverts with Deep Corrugations, and		1.50	0.90
Fiberglass Culverts		1.30	0.90
o Thermoplastic Culverts		1.95	0.90
o All others			
<i>ES</i> : Earth Surcharge		1.50	0.75

Table 3.4.1-3—Load Factors for Permanent Loads Due to Superimposed Deformations, γ_p

Bridge Component	<i>PS</i>	<i>CR, SH</i>
Superstructures—Segmental	1.0	See γ_p for <i>DC</i> , Table 3.4.1-2
Concrete Substructures supporting Segmental Superstructures (see 3.12.4, 3.12.5)		
Concrete Superstructures—non-segmental	1.0	1.0
Substructures supporting non-segmental Superstructures using I_g	0.5	0.5
	using $I_{effective}$	1.0
Steel Substructures	1.0	1.0

Table 3.4.1-4—Load Factors for Live Load for Service III Load Combination, γ_{LL}

Component	γ_{LL}
Prestressed concrete components designed using the refined estimates of time-dependent losses as specified in Article 5.9.5.4 in conjunction with taking advantage of the elastic gain	1.0
All other prestressed concrete components	0.8

Table 3.4.1-5—Load Factors for Permanent Loads Due to Foundation Deformations, γ_{SE}

Foundation Deformation and Deformation Estimation Method	SE
Immediate Settlement	
• Hough method	1.00
• Schmertmann method	1.25
• Local method	*
Consolidation settlement	1.00
Lateral Deformation	
• Soil-structure interaction method (P-y or Strain Wedge)	1.00
• Local method	*
*To be determined by the owner based on local geologic conditions.	

3.16—REFERENCES

•
•

•
•

Kulicki, J. M. and D. Mertz. 2006. “Evolution of Vehicular Live Load Models During the Interstate Design Era and Beyond, in: 50 Years of Interstate Structures: Past, Present and Future”, *Transportation Research Circular*, E-C104, Transportation Research Board, National Research Council, Washington, DC.

Kulicki^[NCS2], J., W. Wassef, D. Mertz, A. Nowak, N. Samtani, and H. Nassif. 2015. *Bridges for Service Life Beyond 100 Years: Service Limit State Design*. SHRP 2 Report S2-R19B-RW-1, SHRP2 Renewal Research, Transportation Research Board, National Research Council, The National Academies, Washington, D.C.

Larsen, D. D. 1983. “Ship Collision Risk Assessment for Bridges.” In Vol. 1, *International Association of Bridge and Structural Engineers Colloquium*. Copenhagen, Denmark, pp. 113–128.

•
•
•

Sabatini, P. J., D. G. Pass, and R. C. Bachus. 1999. *Geotechnical Engineering Circular No. 4—Ground Anchors and Anchored Systems*, Federal Highway Administration, Report No. FHWA-SA-99-015. NTIS, Springfield, VA.

Samtani, N. and J. Kulicki. 2016. *Incorporation of Foundation Deformations in AASHTO LRFD Bridge Design Process*. SHRP2 Solutions. American Association of State Highway and Transportation Officials. Washington, DC.

Saul, R. and H. Svensson. 1980. “On the Theory of Ship Collision Against Bridge Piers.” In *IABSE Proceedings*, February 1980, pp. 51–82.

Proposed Modifications to Section 10

TABLE OF CONTENTS

•
•
•
•
•
•

10.5—LIMIT STATES AND RESISTANCE FACTORS	10-xx
10.5.1—General	10-xx
10.5.2—Service Limit States.....	10-xx
10.5.2.1—General.....	10-xx
10.5.2.2—Tolerable Movements and Movement Criteria	10-xx
10.5.2.2.1—General	10-xx
10.5.2.2.2— <u>Factored Relevant Total Settlement, S_{fr}, and Factored Angular Distortion, A_{df}</u>	<u>10-xx</u>
10.5.2.3—Overall Stability	10-xx

•
•
•
•
•

10.6.2—Service Limit State Design10-xx

10.6.2.1—General.....10-xx

10.6.2.2—Tolerable Movements10-xx

10.6.2.3—Loads.....10-xx

10.6.2.4—Settlement Analyses10-xx

10.6.2.4.1—General10-xx

10.6.2.4.2—Settlement of Footings on Cohesionless Soils.....10-xx

10.6.2.4.2a—General.....10-xx

10.6.2.4.2b— Elastic Half-space Method10-xx

10.6.2.4.2c—Hough Method.....10-xx

10.6.2.4.2d—Schmertmann Method.....10-xx

10.6.2.4.2e—Local Method10-xx

10.6.2.4.3—Settlement of Footings on Cohesive Soils10-xx

-
-
-
-
-

APPENDIX A10—SEISMIC ANALYSIS AND DESIGN OF FOUNDATIONS

A10.1—Investigation	Error! Bookmark not defined.
A10.2—Foundation Design	Error! Bookmark not defined.
A10.3—Special Pile requirements	Error! Bookmark not defined.

APPENDIX B10—CONSIDERATION OF FOUNDATION DEFORMATIONS IN BRIDGE DESIGN

APPENDIX C10—STEP-BY-STEP PROCEDURES FOR THE CONSTRUCTION-POINT AND S_r-0 CONCEPTS FOR ESTIMATING BRIDGE SETTLEMENTS FOR BRIDGE DESIGN

C10.1—Construction-Point Concept	Error! Bookmark not defined.
C10.2— S_r-0 Concept.....	Error! Bookmark not defined.
C10.3—Step-by-Step Procedures.....	Error! Bookmark not defined.

•
•
•
•
•
•

10.3—NOTATION

A_{cs}	=	cross-sectional area of steel casing considering reduction for threads (in. ²) (10.9.3.10.3a)
A_{df}	=	<u>factored angular distortion (10.5.2.2.2)</u>
A_g	=	cross-sectional area of grout within micropile (in. ²) (10.9.3.10.3a)
•		
•		
B	=	footing width; pile group width; pile diameter (ft) (10.6.1.3) (10.7.2.3.2) (10.7.2.4)
B_f	=	<u>least width of footing (10.6.2.4.2b)</u>
B'	=	effective footing width (ft) (10.6.1.3)
C_f	=	<u>correction factor to incorporate the effect of strain relief due to embedment (10.6.2.4.2b)</u>
C_2	=	<u>correction factor to incorporate time-dependent (creep) increase in settlement for t (years) after construction (10.6.2.4.2b)</u>
C_α	=	secondary compression index, void ratio definition (dim) (10.4.6.3)
•		
•		
d_q	=	correction factor to account for the shearing resistance along the failure surface passing through cohesionless material above the bearing elevation (dim) (10.6.3.1.2a)
E	=	modulus of elasticity of pile material (ksi) (10.7.3.8.2); <u>elastic modulus of layer i based on guidance provided in Table C10.4.6.3-1 (10.6.2.4.2b)</u>
E_d	=	developed hammer energy (ft-lb) (10.7.3.8.5)
•		
•		
I_w	=	weak axis moment of inertia for a pile (ft ⁴) (10.7.3.13.4)
I_ϵ	=	<u>strain influence factor from Figure 10.6.2.4.2c-1a</u>
i_σ i_q i_γ	=	load inclination factors (dim) (10.6.3.1.2a)
•		
•		
L_b	=	micropile bonded length (ft) (10.9.3.5.2)
L_f	=	<u>length of footing (10.6.2.4.2b)</u>
L_i	=	depth to middle of length interval at the point considered (ft) (10.7.3.8.6g)
L_p	=	micropile casing plunge length (ft) (10.9.3.10.4)
L_ϵ	=	<u>bridge span length over which A_{df} is computed (10.5.2.2.2)</u>
•		
•		
S	=	<u>settlement (ft) (Appendix C10)</u>
S_c	=	primary consolidation settlement (ft) (10.6.2.4.1)
$S_{c(1-D)}$	=	single dimensional consolidation settlement (ft) (10.6.2.4.3)
S_e	=	elastic settlement (ft) (10.6.2.4.1)

S_f	=	foundation relevant total settlement (ft) (10.5.2.2.2)
S_s	=	secondary settlement (ft) (10.6.2.4.1)
S_t	=	total settlement (ft) (10.6.2.4.1)
S_{tp}	=	total foundation settlement using permanent loads in the Service I load combination (ft) (10.5.2)
S_{tr}	=	total foundation settlement using permanent loads prior to construction of bridge superstructure in the Service I load combination (ft) (10.5.2.2.2)
S_{tr}	=	relevant total foundation settlement defined as $S_{tr} - S_{tp}$ (10.5.2.2.2)
S_u	=	undrained shear strength (ksf) (10.4.6.2.2)
.		
.		
T	=	time factor (dim) (10.6.2.4.3)
t	=	time for a given percentage of one-dimensional consolidation settlement to occur (yr) (10.6.2.4.3); time t from completion of construction to date under consideration for evaluation of C_2 (yrs) (10.6.2.4.2b)
t_1, t_2	=	arbitrary time intervals for determination of secondary settlement, S_s (yr) (10.6.2.4.3)
.		
.		
W_{TI}	=	vertical movement at the head of the drilled shaft (in.) (C10.8.3.5.4d)
X	=	width or smallest dimension of pile group (ft) (10.7.3.9); a factor used to determine the value of elastic modulus (10.6.2.4.2b)
Y	=	length of pile group (ft) (10.7.3.9)
.		
.		
γ_p	=	load factor for downdrag (C10.7.3.7)
γ_{SF}	=	load factor for settlement (10.5.2.2.2)
ΔH_i	=	elastic settlement of layer i (ft) (10.6.2.4.2)
δ	=	elastic deformation of pile (in.); friction angle between foundation and soil (degrees) (C10.7.3.8.2) (10.7.3.8.6f); foundation deformation (rad. or in.) (C10.5.2.2.2, Appendix C10)
δ_f	=	factored deformation (rad. or in.) (Appendix C3)
ΔJ_i	=	elastic spring stiffness of layer i (ft/kip) (10.6.2.4.2)
Δ	=	differential settlement between two bridge support elements spaced at a distance of L_s (ft) (10.5.2.2)
Δ_f	=	factored differential settlement (10.5.2.2.2)
ΔJ_i	=	elastic spring stiffness of layer i (ft/ksf) (10.6.2.4.2d)
Δp	=	net uniform applied stress (load intensity) at the foundation depth (Figure 10.6.2.4.2c-1b)
.		
.		
.		
.		
.		

-
-
-
-
-
-

10.5—LIMIT STATES AND RESISTANCE FACTORS

10.5.1—General

The limit states shall be as specified in Article 1.3.2; foundation-specific provisions are contained in this Section.

Foundations shall be proportioned so that the factored resistance is not less than the effects of the factored loads specified in Section 3.

10.5.2—Service Limit States

10.5.2.1—General

Foundation design at the service limit state shall include:

- Settlements,
- Horizontal movements,
- Overall stability, and
- Scour at the design flood.

Consideration of foundation movements shall be based upon structure tolerance to total and differential movements, rideability and economy. Foundation movements shall include all movement from settlement, horizontal movement, and rotation.

Bearing resistance estimated using the presumptive allowable bearing pressure for spread footings, if used, shall be applied only to address the service limit state.

The foundation movements should be translated to the deck elevation to evaluate the effect of such movements on the superstructure. In this process, deformations of the substructure, i.e., elements between foundation and superstructure, should be added to foundation deformations as appropriate.

C10.5.2.1

In bridges where the superstructure and substructure are not integrated, settlement corrections can be made by jacking and shimming bearings. Article 2.5.2.3 requires jacking provisions for these bridges.

The cost of limiting foundation movements should be compared with the cost of designing the superstructure so that it can tolerate larger movements or of correcting the consequences of movements through maintenance to determine minimum lifetime cost. The Owner may establish more stringent criteria.

The design flood for scour is defined in Article 2.6.4.4.2, and is specified in Article 3.7.5 as applicable at the service limit state.

Presumptive bearing pressures were developed for use with working stress design. These values may be used for preliminary sizing of foundations, but should generally not be used for final design. If used for final design, presumptive values are only applicable at service limit states.

10.5.2.2—Tolerable Movements and Movement Criteria

10.5.2.2.1—General

Foundation movement criteria shall be consistent with the function and type of structure, anticipated service life, and consequences of unacceptable movements on structure performance. Foundation movement shall include vertical, horizontal, and rotational movements. The tolerable movement criteria shall be established by either empirical procedures or structural analyses, or by consideration of both.

Foundation settlement shall be investigated using all applicable loads in the Service I Load Combination specified in Table 3.4.1-1. Transient loads may be omitted from settlement analyses for foundations bearing on or in cohesive soil deposits that are subject to time-dependent consolidation settlements.

All applicable service limit state load combinations in Table 3.4.1-1 shall be used for evaluating horizontal movement and rotation of foundations.

Horizontal movement criteria should be established at the top of the foundation based on the tolerance of the structure to lateral movement, with consideration of the column length and stiffness.

10.5.2.2.2—Assessment of Differential Settlement and Its Effects

Determination of the relevant total foundation settlement should include consideration of how and when settlement occurs during the structure construction process and the uncertainty of the settlement prediction. As a minimum, settlement that occurs after placement of the foundation and substructure elements, assessed using the Construction-Point approach, shall be considered the relevant total settlement when assessing the additional load force effects applied to the superstructure due to differential settlement between piers, foundation elements or non-uniform settlement across a foundation element.

Uncertainty in the settlement estimate shall be

C10.5.2.2.1

Experience has shown that bridges can and often do accommodate more movement and/or rotation than traditionally allowed or anticipated in design. Creep, relaxation, and redistribution of force effects accommodate these movements. Some studies have been made to synthesize apparent response. These studies indicate that angular distortions between adjacent foundations greater than 0.008 radians in simple spans and 0.004 radians in continuous spans should not be permitted in settlement criteria (Moulton et al., 1985; DiMillio, 1982; Barker et al., 1991; Samtani et al. 2010). Other angular distortion limits may be appropriate after consideration of:

- cost of mitigation through larger foundations, realignment or surcharge,
- rideability,
- vertical clearance,
- tolerable limits of deformation of other structures associated with a bridge, e.g., approach slabs, wing walls, pavement structures, drainage grades, utilities on the bridge, etc.
- roadway drainage,
- aesthetics, and
- safety.

Rotation movements should be evaluated at the top of the substructure unit in plan location and at the deck elevation.

Tolerance of the superstructure to lateral movement will depend on bridge seat or joint widths, bearing type(s), structure type, and load distribution effects.

C10.5.2.2.2

The application of γ_{SF} is illustrated in the flowchart in Appendix B10. Details of how to conduct the construction-point and S_0 approaches are provided in Appendix C10. The recommended procedure is to factor the deformations and evaluate the effect on the structure using the factored deformations. If a structural analysis of factored deformations is performed, the resulting force effects are already factored, and these results are used directly in the appropriate load combinations in Table 3.4.1-1. An additional application of γ_{SF} in Table 3.4.1-1 is not required since the force effects are already factored.

Note that the flow chart in Appendix B10 uses the

determined as follows:

$$S_f = \gamma_{SF}(S_{fT})$$

where,

$$S_f = \text{factored relevant total foundation total settlement (ft)}$$

$$S_{fT} = \text{unfactored relevant total foundation settlement (ft)}$$

$$\gamma_{SF} = \text{SE load factor value selected from Table 3.4.1-5 3.4.1-4 based on the method used to estimate the settlement.}$$

For assessing the differential settlement within each bridge span, the maximum differential settlement between adjacent piers should be assessed using the S_f -0 approach, in which it is assumed that the bridge pier with the smallest factored relevant total settlement S_f has zero settlement while the other pier has the factored estimated relevant total settlement S_f [NCS1].

The differential settlement across each bridge pier (i.e., in transverse direction) should be performed based on consideration of bridge width and stiffness. If the distance between support elements in the transverse direction is less than one-half of the bridge width at that line of support elements, then the angular distortion may be computed based on the difference between the factored relevant settlement between the support points rather than assuming one of the support points has zero total settlement.

10.5.2.3—Overall Stability

The evaluation of overall stability of earth slopes with or without a foundation unit shall be investigated at the service limit state as specified in Article 11.6.2.3.

10.5.2.4—Abutment Transitions

Vertical and horizontal movements caused by embankment loads behind bridge abutments shall be investigated.

symbol δ that is general and applies to any type of deformation. When the flow chart is used for settlement, the the symbol “S” may be substituted for δ . can be substituted with S . Similar substitutions can be performed for other types of foundation deformations, e.g., if the flow chart is used for lateral deformation of a deep foundation, then the symbol “y” may be substituted for δ .

The “legacy” design approach of not considering γ_{SF} and not using the S_f -0 approach to estimate differential settlement across a bridge span when total and differential settlements are small (e.g., less than 1 inch [NCS2]) may still be used if:

- the geomaterials at a site are well understood, and
- past experience shows that for the considered foundation and service bearing pressure results in acceptable foundation deformations with minimal structural or geometric consequences.

C10.5.2.4

Settlement of foundation soils induced by embankment loads can result in excessive movements of substructure elements. Both short and long term settlement potential should be considered.

Settlement of improperly placed or compacted backfill behind abutments can cause poor rideability and a possibly dangerous bump at the end of the bridge. Guidance for proper detailing and material requirements for abutment backfill is provided in Cheney and Chassie Samtani and Nowatzki (20096).

Lateral earth pressure behind and/or lateral squeeze below abutments can also contribute to lateral movement of abutments and should be investigated, if applicable.

-
-
-

10.6.2.4—Settlement Analyses

10.6.2.4.1—General

Foundation settlements should be estimated using computational methods based on the results of laboratory or insitu testing, or both. The soil parameters used in the computations should be chosen to reflect the loading history of the ground, the construction sequence, and the effects of soil layering.

Both total and differential settlements, including time dependant effects, shall be considered.

Total settlement, including elastic, consolidation, and secondary components may be taken as:

$$S_t = S_e + S_c + S_s \quad (10.6.2.4.1-1)$$

where:

S_e = elastic settlement (ft)

S_c = primary consolidation settlement (ft)

S_s = secondary settlement (ft)

The effects of the zone of stress influence, or vertical stress distribution, beneath a footing shall be considered in estimating the settlement of the footing.

Spread footings bearing on a layered profile consisting of a combination of cohesive soil, cohesionless soil and/or rock shall be evaluated using an appropriate settlement estimation procedure for each layer within the zone of influence of induced stress beneath the footing.

C10.6.2.4.1

Elastic, or immediate, settlement is the instantaneous deformation of the soil mass that occurs as the soil is loaded. The magnitude of elastic settlement is estimated as a function of the applied stress beneath a footing or embankment. Elastic settlement is usually small and neglected in design, but where settlement is critical, it is the most important deformation consideration in cohesionless soil deposits and for footings bearing on rock. For footings located on over-consolidated clays, the magnitude of elastic settlement is not necessarily small and should be checked.

In a nearly saturated or saturated cohesive soil, the pore water pressure initially carries the applied stress. As pore water is forced from the voids in the soil by the applied load, the load is transferred to the soil skeleton. Consolidation settlement is the gradual compression of the soil skeleton as the pore water is forced from the voids in the soil. Consolidation settlement is the most important deformation consideration in cohesive soil deposits that possess sufficient strength to safely support a spread footing. While consolidation settlement can occur in saturated cohesionless soils, the consolidation occurs quickly and is normally not distinguishable from the elastic settlement.

Secondary settlement, or creep, occurs as a result of the plastic deformation of the soil skeleton under a constant effective stress. Secondary settlement is of principal concern in highly plastic or organic soil deposits. Such deposits are normally so obviously weak and soft as to preclude consideration of bearing a spread footing on such materials.

The principal deformation component for footings on rock is elastic settlement, unless the rock or included discontinuities exhibit noticeable time-dependent behavior.

To avoid overestimation, relevant settlements should be evaluated using the construction-point concept noted in Samtani and Kulicki (2016) and Appendix C10.

For guidance on vertical stress distribution for complex footing geometries, see Poulos and Davis (1974) or Lambe and Whitman (1969).

Some methods used for estimating settlement of footings on sand include an integral method to account for the effects of vertical stress increase variations. For guidance regarding application of these procedures, see Gifford et al. (1987).

The distribution of vertical stress increase below circular or square and long rectangular footings, i.e., where $L > 5B$, may be estimated using Figure 10.6.2.4.1-1.

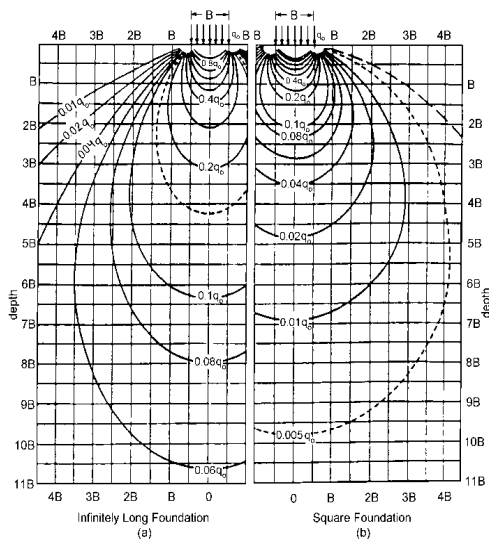


Figure 10.6.2.4.1-1—Boussinesq Vertical Stress Contours for Continuous and Square Footings Modified after Sowers (1979)

10.6.2.4.2—Settlement of Footings on Cohesionless Soils

10.6.2.4.2a—General

The settlement of spread footings bearing on cohesionless soil deposits shall be estimated as a function of effective footing width and shall consider the effects of footing geometry and soil and rock layering with depth.

Settlements of footings on cohesionless soils shall be estimated using elastic theory or calibrated empirical procedures. [TA3]

C10.6.2.4.2a

Although methods are recommended for the determination of settlement of cohesionless soils, experience has indicated that settlements can vary considerably in a construction site, and this variation may not be predicted by conventional calculations.

Settlements of cohesionless soils occur rapidly, essentially as soon as the foundation is loaded. Therefore, the total settlement under the service loads may not be as important as the incremental settlement between intermediate load stages. For example, the total and differential settlement due to loads applied by columns and cross beams is generally less important than the total and differential settlements due to girder placement and casting of continuous concrete decks.

Generally conservative settlement estimates may be obtained using the elastic half-space procedure, or the empirical methods by Hough and Schmertmann. Additional information regarding the accuracy of the

methods described herein is provided in Gifford et al. (1987), and Kimmerling (2002), ~~and Samtani and Notwazki (2006), and Samtani and Allen (2017).~~ [TA4] This information, in combination with local experience and engineering judgment, should be used when determining the estimated settlement for a structure foundation, as there may be cases, such as attempting to build a structure grade high to account for the estimated settlement, when overestimating the settlement magnitude could be problematic.

Details of other procedures can be found in textbooks and engineering manuals, including:

- Terzaghi and Peck (1967)
- Sowers (1979)
- U.S. Department of the Navy (1982)
- D'Appolonia (Gifford et al., 1987)—This method includes consideration for over-consolidated sands.
- Tomlinson (1986)
- Gifford et al. (1987)

10.6.2.4.2b—Elastic Half-space Method

The elastic half-space method assumes the footing is flexible and is supported on a homogeneous soil of infinite depth. The elastic settlement of spread footings, in feet, by the elastic half-space method shall be estimated as:

$$S_e = \frac{q_o \left(1 - \nu^2\right) \sqrt{A'}}{144 E_s \beta_z} \quad (10.6.2.4.2b-1)$$

where:

- q_o = applied vertical stress (ksf)
- A' = effective area of footing (ft²)
- E_s = Young's modulus of soil taken as specified in Article 10.4.6.3 if direct measurements of E_s are not available from the results of in situ or laboratory tests (ksi)
- β_z = shape factor taken as specified in Table 10.6.2.4.2b-1 (dim)
- ν = Poisson's Ratio, taken as specified in Article 10.4.6.3 if direct measurements of ν are not available from the results of in situ or laboratory tests (dim)

C10.6.2.4.2b

For general guidance regarding the estimation of elastic settlement of footings on sand, see Gifford et al. (1987), and Kimmerling (2002), and Samtani and Notwazki (2006).

The stress distributions used to calculate elastic settlement assume the footing is flexible and supported on a homogeneous soil of infinite depth. The settlement below a flexible footing varies from a maximum near the center to a minimum at the edge equal to about 50 percent and 64 percent of the maximum for rectangular and circular footings, respectively. The settlement profile for rigid footings is assumed to be uniform across the width of the footing.

Spread footings of the dimensions normally used for bridges are generally assumed to be rigid, although the actual performance will be somewhere between perfectly rigid and perfectly flexible, even for relatively thick concrete footings, due to stress redistribution and concrete creep.

The accuracy of settlement estimates using elastic theory are strongly affected by the selection of soil modulus and the inherent assumptions of infinite elastic half space. Accurate estimates of soil moduli are difficult to obtain because the analyses are based on only a single value of soil modulus, and Young's modulus varies with depth as a function of overburden stress. Therefore, in selecting an appropriate value for soil modulus, consideration should be given to the influence of soil layering, bedrock at a shallow depth,

Unless E_s varies significantly with depth, E_s should be determined at a depth of about 1/2 to 2/3 of B below the footing, where B is the footing width. If the soil modulus varies significantly with depth, a weighted average value of E_s should be used.

Table 10.6.2.4.2b-1—Elastic Shape and Rigidity Factors, EPRI (1983)

L/B	Flexible, β_z (average)	β_z Rigid
Circular	1.04	1.13
1	1.06	1.08
2	1.09	1.10
3	1.13	1.15
5	1.22	1.24
10	1.41	1.41

[TA5]

10.6.2.4.2c—Hough Method

Estimation of spread footing settlement on cohesionless soils by the empirical Hough method shall be determined using Eqs. 10.6.2.4.2c-2 and 10.6.2.4.2c-3. *SPT* blow counts shall be corrected as specified in Article 10.4.6.2.4 for depth, i.e. overburden stress, before correlating the *SPT* blow counts to the bearing capacity index, C' .

$$S_e = \sum_{i=1}^n \Delta H_i \quad (10.6.2.4.2c-1)$$

in which:

$$\Delta H_i = H_c \frac{1}{C'} \log \left(\frac{\sigma'_o + \Delta \sigma_v}{\sigma'_o} \right) \quad (10.6.2.4.2c-2)$$

where:

n = number of soil layers within zone of stress influence of the footing

ΔH_i = elastic settlement of layer i (ft)

H_c = initial height of layer i (ft)

C' = bearing capacity index from Figure 10.6.2.4.2c-1 (dim)

σ'_o = initial vertical effective stress at the midpoint of

and adjacent footings.

For footings with eccentric loads, the area, A' , should be computed based on reduced footing dimensions as specified in Article 10.6.1.3.

C10.6.2.4.2c

The Hough method was developed for normally consolidated cohesionless soils.

The Hough method has several advantages over other methods used to estimate settlement in cohesionless soil deposits, including express consideration of soil layering and the zone of stress influence beneath a footing of finite size.

The subsurface soil profile should be subdivided into layers based on stratigraphy to a depth of about three times the footing width. The maximum layer thickness should be about 10 ft.

While Cheney and Chassie (2000), and Hough (1959), did not specifically state that the *SPT* N values should be corrected for hammer energy in addition to overburden pressure, due to the vintage of the original work, hammers that typically have an efficiency of approximately 60 percent were in general used to develop the empirical correlations contained in the method. If using *SPT* hammers with efficiencies that differ significantly from this 60 percent value, the N values should also be corrected for hammer energy, in effect requiring that N_{160} be used (Samtani and Nowatzki, 2006).

Studies conducted by Gifford et al. (1987) and Samtani and Nowatzki (2006) indicate that Hough's procedure is more conservative, but has less prediction variability, than the Schmertmann Method. However, this difference is mostly taken into account through the load factor, γ_{SE} , since it has been calibrated using reliability theory (Kulicki, et al. 2015; Samtani and Kulicki, 2016; and Samtani and Allen (2017) Samtani/Allen222). [TA6]

layer i (ksf)

$\Delta\sigma_v =$ increase in vertical stress at the midpoint of layer i (ksf)

In Figure 10.6.2.4.2-1, N_1 shall be taken as N_{160} , Standard Penetration Resistance, N (blows/ft), corrected for overburden pressure as specified in Article 10.4.6.2.4..

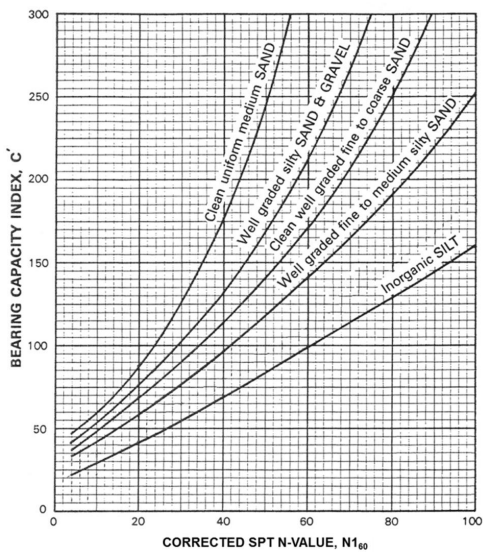


Figure 10.6.2.4.2c-1—Bearing Capacity Index versus Corrected SPT (modified from Cheny and Chassie, 2000; Samtani and Nowatzki, 2006, modified from after Hough, 1959)

10.6.2.4.2d—Schmertmann Method

Estimation of spread footing immediate settlement, S_p , on cohesionless soils by the empirical Schmertmann method shall be made using Eq. 10.6.2.4.2d-1.

$$S_i = C_1 C_2 \Delta p \sum_{i=1}^n \frac{\Delta J_i}{E} \quad (10.6.2.4.2d-1)$$

in which:

The Hough method is applicable to cohesionless soil deposits. The “Inorganic Silt” curve should generally not be applied to soils that exhibit plasticity because N-values in such soils tend to be highly variable. The settlement characteristics of cohesive soils that exhibit plasticity should be investigated using undisturbed samples and laboratory consolidation tests as prescribed in Article 10.6.2.4.3.

C10.6.2.4.2d

Background information for Schmertmann, *et al.* (1978) in the format as presented here can be found in Samtani and Nowatzki (2006).

The variables in the equation for ΔJ_i (Equation 2) require specific units for H_c (ft) and E (provided in Table C10.4.6.3-1) is in ksi. This results in the units for ΔJ_i being ft/kip. Furthermore, in Equation 1, Δp units must be ksf. [TA9][NCS10]

For C_2 correction factor the time duration, t , in Eq. 10.6.2.4.2d-4 is set to 0.1 years to evaluate the settlement immediately after construction, i.e., $C_2 = 1$.

$$\Delta J_i = H_c \left(\frac{I_z}{144 X E} \right) \quad (10.6.2.4.2d-2)$$

$$C_1 = 1 - 0.5 \left(\frac{P_o}{\Delta p} \right) \geq 0.5 \quad (10.6.2.4.2d-3)$$

$$C_2 = 1 + 0.2 \log_{10} \left(\frac{t}{0.1} \right) \quad (10.6.2.4.2d-4)$$

where:

ΔJ_i = elastic spring stiffness of layer i
(ft/kipksf) [TA7] [NCS8]

H_c = height of compressible soil layer i (ft)

I_z = strain influence factor from Figure 10.6.2.4.2d-1a. The dimension B_f represents the least lateral dimension of the footing after correction for eccentricities, i.e. use least lateral effective footing dimension. The strain influence factor is a function of depth and is obtained from the strain influence diagram. The strain influence diagram is constructed for the axisymmetric case ($L_f/B_f = 1$) and the plane strain case ($L_f/B_f \geq 10$) as shown in Figure 10.6.2.4.2d-1a. The strain influence diagram for intermediate conditions should be determined by simple linear interpolation.

n = number of soil layers within the zone of strain influence (strain influence diagram).

Δp = net uniform applied stress (load intensity) at the foundation depth (see Figure 10.6.2.4.2d-1b) (ksf).

E = elastic modulus of layer i based on guidance provided in Table C10.4.6.3-1 (ksi).

X = a factor used to determine the value of elastic modulus. If the value of elastic modulus is based on correlations with NI_{60} -values or q_c from Table C10.4.6.3-1, then values of X shall be taken as follows:

$X = 1.25$ for axisymmetric case ($L_f/B_f = 1$)

If long-term creep deformation of the soil is suspected then an appropriate time duration, t , should be used in the computation of C_2 . Creep deformation is not the same as consolidation settlement. This factor can have an important influence on the reported settlement since it is included in Eq. 10.6.2.4.2d-1 as a multiplier. For example, the C_2 factor for time durations of 0.1 yrs, 1 yr, 10 yrs and 50 yrs are 1.0, 1.2, 1.4 and 1.54, respectively. In cohesionless soils and unsaturated fine-grained cohesive soils with low plasticity, time durations of 0.1 yr and 1 yr, respectively, are generally appropriate and sufficient for cases of static loads.

$X = 1.75$ for plane strain case ($L_f/B_f \geq 10$)

Use interpolation for footings with values of L_f/B_f between 1 and 10.

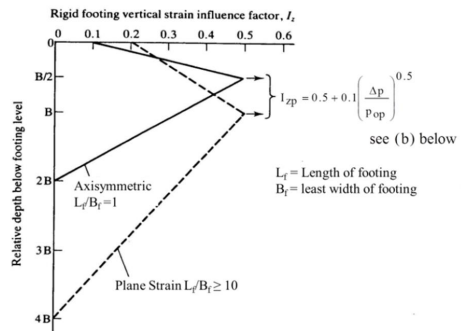
If the value of elastic modulus is estimated based on the range of elastic moduli in the upper half of Table C10.4.6.3-1, or based on other sources, such as in-situ testing (e.g., pressuremeter), use $X = 1.0$.

C_1 = correction factor to incorporate the effect of strain relief due to embedment

p_o = effective in-situ overburden stress at the foundation depth and Δp is the net foundation pressure as shown in Figure 10.6.2.4.2d-1b (ksf).

C_2 = correction factor to incorporate time-dependent (creep) increase in settlement for time t after construction

t = time t from completion of construction to date under consideration for evaluation of C_2 (yrs)



(a)

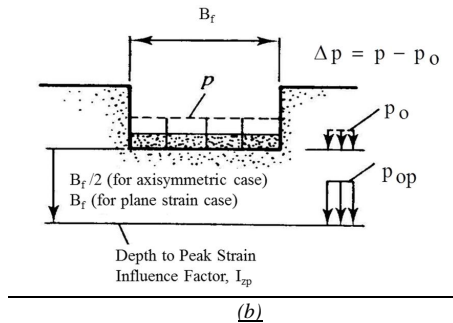


Figure 10.6.2.4.2d-1—(a) Simplified vertical strain influence factor distributions, (b) Explanation of pressure terms in equation for I_{sp} (Samtani and Notatzki, 2006, after Schmertmann, et al., 1978).

The C_2 parameter shall not be used to estimate time-dependent consolidation settlements. Where consolidation settlement can occur within the depth of the strain distribution diagram, the magnitude of the consolidation settlement shall be estimated as per Article 10.6.2.4.3 and added to the immediate settlement of other layers within the strain distribution diagram where consolidation settlement may not occur.

10.6.2.4.2e—Local Method

Use of methods based on local geologic conditions and calibration shall be used subject to require approval from the Owner.

C10.6.2.4.2e

Calibration of local methods should be based on processes as described in SHRP 2 R19B program report (Kulicki et al., 2015) and Samtani and Kulicki (2016) [TA11] [NCS12]

10.10—REFERENCES

-
-
-
- Kulhawy, F.H. and Y-R Chen. 2007. "Discussion of 'Drilled Shaft Side Resistance in Gravelly Soils' by Kyle M. Rollins, Robert J. Clayton, Rodney C. Mikesell, and Bradford C. Blaise," *Journal of Geotechnical and Geoenvironmental Engineering*, ASCE, Vol. 133, No. 10, pp. 1325–1328.

Kulicki [NCS13], J., W. Wassef, D. Mertz, A. Nowak, N. Samtani, and H. Nassif. 2015. "Bridges for Service Life Beyond 100 Years: Service Limit State Design." *SHRP 2 Report S2-R19B-RW-1*, SHRP2 Renewal Research, Transportation Research Board, National Research Council, The National Academies, Washington, D.C.

Kyfor, Z. G., A. R. Schnore, T. A. Carlo, and P. F. Bailey. 1992. *Static Testing of Deep Foundations*, FHWA-SA-91-042, Federal Highway Administration, Office of Technology Applications, U. S. Department of Transportation, Washington D. C., p. 174.

-
-
-

Sabatini, P. J., R. C. Bachus, P. W. Mayne, J. A. Schneider, and T. E. Zettler. 2002. *Geotechnical Engineering Circular 5 (GEC5)—Evaluation of Soil and Rock Properties*, FHWA-IF-02-034. Federal Highway Administration, U.S. Department of Transportation, Washington, DC.

Samtani, N. C., and Nowatzki, E. A. 2006. *Soils and Foundations*, FHWA NHI-06-088 and FHWA NHI 06-089, Federal Highway Administration, U.S. Department of Transportation, Washington, DC.

Samtani, N. C., Nowatzki, E. A., and Mertz, D.R. 2010. *Selection of Spread Footings on Soils to Support Highway Bridge Structures*, FHWA-RC/TD-10-001, Federal Highway Administration, Resource Center, Matteson, IL

Samtani, N. and J. Kulicki. 2016. *Incorporation of Foundation Deformations in AASHTO LRFD Bridge Design Process*. SHRP2 Solutions. American Association of State Highway and Transportation Officials. Washington, DC.

Samtani, N. and T. Allen. 2017. *Expanded Database and Service Limit State Calibration for Immediate Settlement of Spread Footings*. SHRP2 Solutions. American Association of State Highway and Transportation Officials. Washington, DC.

Schmertmann, J. H., Hartman, J. P., and Brown, P. R. 1978. "Improved Strain Influence Factor Diagrams." American Society of Civil Engineers, *Journal of the Geotechnical Engineering Division*, 104 (No. GT8), 1131-1135.



Seed, R. B. and L. F. Harder. 1990. SPT-Based Analysis of Pore Pressure Generation and Undrained Residual Strength. In *Proc., H. B. Seed Memorial Symposium*, Berkeley, CA, May 1990. BiTech Ltd., Vancouver, BC, Canada, Vol. 2, pp. 351–376.

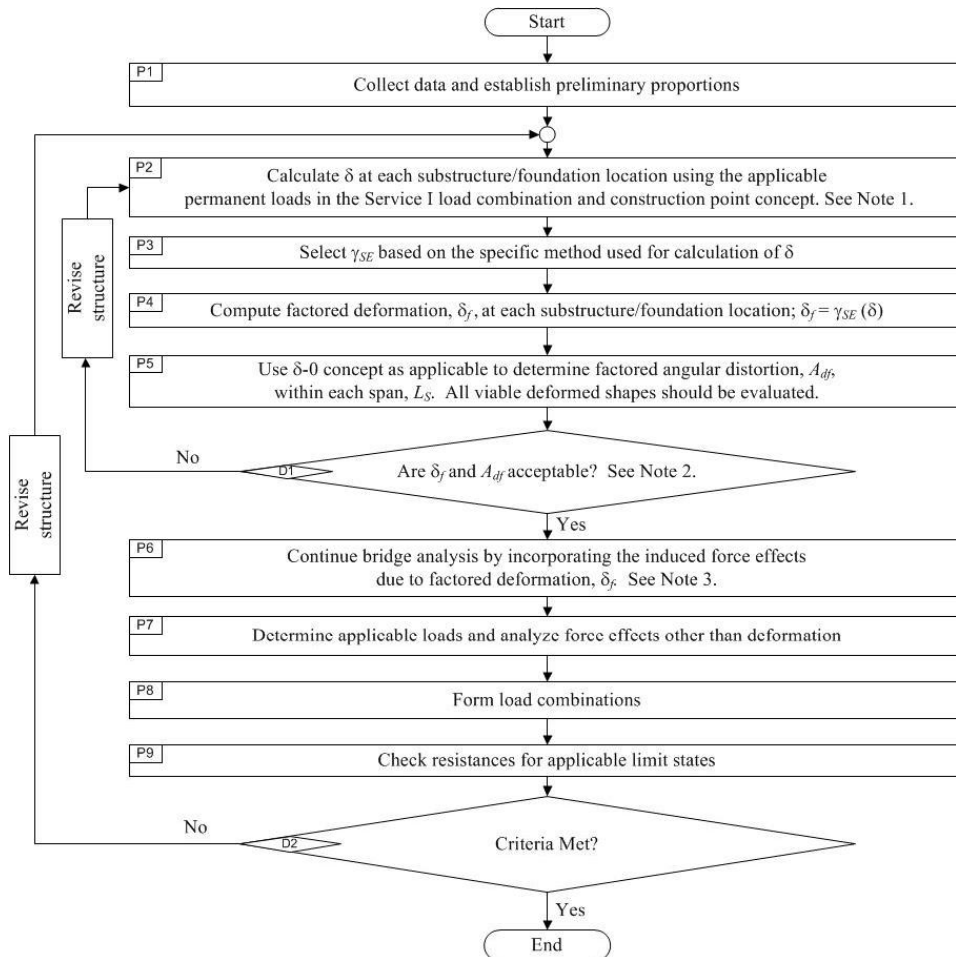
APPENDIX B10—CONSIDERATION OF FOUNDATION DEFORMATIONS IN BRIDGE DESIGN

Previous editions of the AASHTO LRFD Bridge Design Specifications have specified a value of 1.0 be used for γ_{SE} , the load factor for the force effect due to settlement, or be based on project specific information. This load factor was then applied to the extreme combinations of force effects caused by differential settlement between and within substructure units, in accordance with Article 3.12.6. In past design practice, some designers have assumed, based on long-term experience, that these extreme force effects due to differential settlement are not likely to be a controlling factor in the design if the total settlement of the substructure units is small, based on local experience, and in such cases did not need to consider γ_{SE} . This “legacy” design approach may still be used in the current specifications if the geomaterials at a site are well understood and past experience shows that for the considered foundation and service bearing pressure results in acceptable foundation deformations with minimal structural or geometric consequences.

However, the recommended procedure is to factor the deformations and evaluate their effects on the structure using the factored deformations. Figure B10-1 illustrates the design process used for the recommended procedure. This design process is based on Samtani and Kulicki (2016), which includes the method-specific load factor, γ_{SE} , and the construction-point concept or the δ -0 concept. The flow chart applies to any type of foundation deformation and hence the symbol δ is used for deformations. If the flow chart is used for settlement, then the symbol “ S ” may be substituted for δ . Similar substitutions can be performed for other types of foundation deformations, e.g., if the flow chart is used for lateral deformation of a deep foundation, then the symbol “ γ ” may be substituted for δ .

Some of the key points associated with the flow chart are as follows:

1. The process (“P”) related steps are indicated in rectangular boxes (). There are five process boxes labeled P1 to P9.
2. The decision (“D”) related steps are indicated in diamond boxes (). There are two decision boxes labeled D1 and D2.
3. The design proceeds as follows:
 - After the calculation of δ for the indicated loads in box P2 and adjusting them for the construction-point concept, they are scaled (factored) as indicated in box P4 using the method-specific values of γ_{SE} determined in box P2.
 - These factored deformations, δ_f , are used along with the δ -0 concept to calculate the factored angular distortions, A_{df} in box P5.
 - In box D1 the values of δ_f and A_{df} are compared to the applicable criteria. These criteria are geometric, not structural. Note 2 provides additional guidance.
 - If the results are not acceptable the structure is revised and the design process returns to box P2 to evaluate the modified structure.
 - If the results at box D1 are acceptable, the structural force effects from the factored deformations, δ_f , are calculated and carried into box P6 and remaining steps. Note 3 is vital to the correct formulation of load combinations using Table 3.4.1-1.
4. The “Criteria” in box D1 can include any criteria related to bridge design such as deck grades, joint distress, crack control, moment and shear resistance.
5. If all structural and geometric criteria are satisfied in box D2 the design is satisfactory; if not, the structure is modified and the design process returns to box P2.



Note 1: See Appendix C10 for construction point concept. Before performing operations P2 to P6, it may be efficient to run some early design iterations without considering deformations until the proportions of the bridge are well developed and then consider the force effects due to differential deformations.

Note 2: Compare A_{df} to permissible angular distortion criteria and δ_f to permissible values at abutment interfaces and within spans in terms of vertical clearance under bridge. Guidance in Article 10.5.2 may be used to establish permissible values. Owner may establish other permissible values.

Note 3: Note that the γ_{SE} is used to factor the deformations as shown in this flow chart. γ_{SE} also appears in Table 3.4.1-1 (Load Combinations and Load Factors). This does not imply a second application of γ_{SE} in the load combinations but rather it is an acknowledgement that the deformations have already been factored. Use of the factored deformations in a structural analysis program ensures that the output is factored value.

Figure B10-1—Foundation Deformation Procedure Flow Chart (Samtani and Kulicki, 2016)

References

Samtani, N. and J. Kulicki. 2016. *Incorporation of Foundation Deformations in AASHTO LRFD Bridge Design Process*. SHRP2 Solutions. American Association of State Highway and Transportation Officials. Washington, DC.

APPENDIX C10—STEP-BY-STEP PROCEDURES FOR THE CONSTRUCTION- POINT AND S_T -0 CONCEPTS FOR ESTIMATING BRIDGE SETTLEMENTS FOR BRIDGE DESIGN

Determination of relevant total settlement should include consideration of how and when settlement occurs during construction process and uncertainty of the settlement itself. These two factors are addressed by the construction-point concept and S_T -0 concept, respectively.

C10.1 Construction-Point Concept

Foundation deformations should not be estimated as if a weightless bridge structure is instantaneously set into place and all the loads are applied at the same time. In reality, loads are applied gradually as construction proceeds. Consequently, foundation deformations also occur gradually as construction proceeds. There are several critical construction points or stages during construction that should be evaluated separately by the designer. Figure C10-1 shows the critical construction stages (W, X, Y, and Z) and their associated load-settlement behavior for the case of a pier and vertical loads. In this case, the total foundation settlement, S_{tot} , is equal to the settlement corresponding to the total construction load, Z. Thus, $S_{\text{tot}} = S_Z$. The settlements that occur before placement of the superstructure may not be relevant to the design of the superstructure. Thus, the settlements between application of loads X and Z are the most relevant. For continuous-span bridges the settlement, S_X , corresponding to load X may be applicable for computing relevant total settlement, S_T . In this case, the total foundation settlement, S_{tot} , prior to construction of bridge superstructure is equal to the settlement corresponding to Load X. Thus, for this example, $S_T = S_Z - S_X$. Similarly, for simple-span bridges where settlement, S_Y , corresponding to load Y may be applicable for computing relevant total settlement, $S_T = S_Z - S_Y$. Formulation of settlements in a manner shown in Figure C10-1b permits an assessment of settlements up to that point that can affect the bridge superstructure. Although Figure C10-1 illustrates the construction-point concept for the case of a pier, vertical loads and settlements (vertical deformation), the concepts apply to other elements of bridge structure (e.g., abutments), load types (shears, moments, etc.) and deformation types (lateral movements, rotations, etc.).

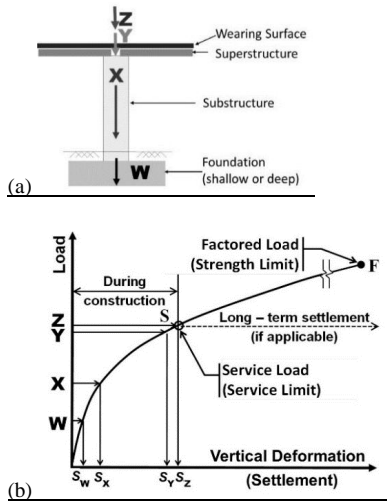


Figure C10-1. Construction-point concept for a bridge pier. (a) Identification of critical construction points, (b) conceptual load-deformation pattern for a given foundation (Kulicki, et. al, 2015; Samtani and Kulicki, 2016).

Long-term settlements as shown by the horizontal dashed line corresponding to the total construction load (Z) in Figure C10-1 should be included as appropriate.

C10.2 S_F -0 Concept

While all analytical methods for estimating settlements have some degree of uncertainty, the uncertainty of the calculated differential settlement is larger than the uncertainty of the calculated total settlement at each of the two support elements used to calculate that differential settlement, e.g., between an abutment and a pier, or between two adjacent piers. The S_F -0 concept is used to account for this uncertainty.

A hypothetical 4-span bridge structure with span lengths, L_{S1} , L_{S2} , L_{S3} and L_{S4} is shown in Figure C10.5.2.2-2 C10-2 to illustrate the application of S_F -0 concept and computation of factored angular distortion. The factored relevant total settlement, S_F , is computed at each support element and the profile of S_F along the bridge is shown by the solid line. In this figure, $S_{F-A1} < S_{F-P1} > S_{F-P2} < S_{F-P3} < S_{F-A2}$. As shown, two viable modes of deformation shapes, Mode 1 and Mode 2, are possible. For each of these two modes, the S_F profile assumed for computation of the factored angular distortion, A_{df} , for each span is represented by the dashed lines. The factored angular distortion within each span is computed as shown for each viable mode as shown in Figure C10-2. The symbols are in accordance with Δ_{fi-j} and A_{dfi-j} where i represents the span number (1 to 4) and j represents the mode (1 and 2).

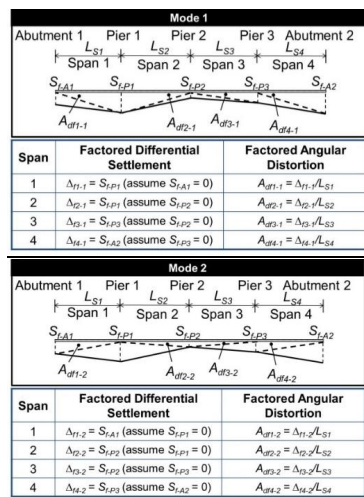


Figure C10-2—Computing Factored Angular Distortion, A_{df} , Based on S_F -0 Concept for a hypothetical 4-span Bridge (Samtani and Kulicki, 2016).

The application of γ_{SF} is illustrated in the flowchart in Appendix B10. The recommended procedure is to factor the deformations and evaluate the effect on the structure using the factored deformations. If a structural analysis of factored deformations is performed, the resulting force effects are already factored and these results are used directly in the appropriate load combinations in Table 3.4.1-1. An additional application of γ_{SF} in Table 3.4.1-1 is not required since the force effects are already factored.

Note that the flow chart in Appendix B10 uses the symbol δ that is general and applies to any type of deformation. When the flow chart is used for settlement, δ can be substituted with S .

C10.3 Step-by-Step Procedures

The following steps should be followed to estimate factored settlement, S_F , and factored angular distortion, A_{df} for the design of the structure and its foundations, where, in the design steps that follow:

S_F = factored relevant foundation total settlement (ft)

S_{ia} = unfactored total foundation settlement using all applicable permanent loads in the Service I load combination (ft)

S_{ip} = unfactored total foundation settlement using all applicable permanent loads prior to construction of bridge superstructure in the Service I load combination (ft)

S_{ir} = unfactored relevant total foundation settlement defined as $S_{ia} - S_{ip}$

1. At each support element, compute factored relevant total foundation settlement for the assumed foundation type (e.g., spread footings, driven piles, drilled shafts, etc.) as follows:
 - a. Determine the unfactored total foundation settlement, S_{ia} , using all applicable permanent loads in the Service I load combination.
 - b. Determine the unfactored total foundation settlement, S_{ip} , prior to construction of bridge superstructure. This settlement would generally be as a result of all applicable substructure loads computed in accordance with permanent loads in the Service I load combination.
 - c. Determine relevant total settlement, S_{ir} as $S_{ir} = S_{ia} - S_{ip}$.
 - d. Determine the factored relevant total settlement, S_f , using Eq. C10.3-1:

$$S_f = \gamma_{SE}(S_{ir}) \quad (C10.3-1)$$

where:

γ_{SE} = SE load factor value selected from Table 3.4.1-43.4.1-5 based on the method used to estimate the settlement.

2. Compute the factored angular distortion within each span using the S_f -0 concept. At a given support element assume that the actual settlement could be as large as the factored relevant total settlement calculated by the chosen method, S_f . At the same time, assume that an adjacent support element does not settle at all. Thus, the factored differential settlement, Δ_f , within a given bridge span is equal to the larger of the factored relevant total settlement at each of two supports of a bridge span. Compute factored angular distortion, A_{df} , as the ratio of the factored differential settlement, Δ_f , to the span length, L_s . Express A_{df} value in radians.

All viable deformation shapes should be evaluated.

If γ_{SE} has already been applied in computation of factored settlement, S_f , as indicated in Step 1d, it should not be applied again during computation of differential settlement or angular distortion.

The value of S_f should be evaluated with respect to the various factors listed in this appendix.

References

Kulicki, J., W. Wassef, D. Mertz, A. Nowak, N. Samtani, and H. Nassif. 2015. "Bridges for Service Life Beyond 100 Years: Service Limit State Design." SHRP 2 Report S2-R19B-RW-1, SHRP2 Renewal Research, Transportation Research Board, National Research Council, The National Academies, Washington, D.C.

Samtani, N. and J. Kulicki. 2016. *Incorporation of Foundation Deformations in AASHTO LRFD Bridge Design Process*. SHRP2 Solutions. American Association of State Highway and Transportation Officials, Washington, DC.

ATTACHMENT 6

Service II, Premature yielding of Steel Structures, Agenda Item
From
the 2015 SCOBS Annual Meeting Agenda

2015 AASHTO BRIDGE COMMITTEE AGENDA ITEM: 12

SUBJECT: LRFD Bridge Design Specifications: Section 3, Articles 3.4.1 and 3.16

TECHNICAL COMMITTEE: T-14 Steel / T-5 Loads

<input checked="" type="checkbox"/> REVISION	<input checked="" type="checkbox"/> ADDITION	<input type="checkbox"/> NEW DOCUMENT
<input checked="" type="checkbox"/> DESIGN SPEC	<input type="checkbox"/> CONSTRUCTION SPEC	<input type="checkbox"/> MOVABLE SPEC
<input type="checkbox"/> MANUAL FOR BRIDGE EVALUATION	<input type="checkbox"/> SEISMIC GUIDE SPEC	<input type="checkbox"/> BRIDGE ELEMENT INSP GUIDE
	<input type="checkbox"/> OTHER	

DATE PREPARED: 7/1/14
DATE REVISED: 9/30/14

AGENDA ITEM:

Item #1

Revise the 9th bullet of Article 3.4.1 as follows:

- Service II—Load combination intended to control yielding of steel structures and slip of slip-critical connections due to vehicular live load. For structures with unique truck loading conditions, such as access roads to ports or industrial sites which might lead to a disproportionate number of permit loads, a site-specific increase in the load factor should be considered.

Item #2

Revise the commentary to Service II in Article C3.4.1 as follows:

This load combination corresponds to the overload provision for steel structures in past editions of the AASHTO Specifications, and it is applicable only to steel structures. From the point of view of load level, this combination is approximately halfway between that used for Service I and Strength I Limit States. An evaluation of WIM data from 31 sites around the country (Kulicki et al., 2014) indicated that the probability of exceeding the load level specified in Table 3.4.1-1 for this limit state could be less than once every six months.

Item #3

Add the following reference to Article 3.16:

Kulicki, J. M., W. G. Wassef, D. R. Mertz, A. S. Nowak, and N. C. Samtani. 2014. Bridges for Service Life Beyond 100 Years: Service Limit State Design, Prepublication Draft. SHRP2, Transportation Research Board of the National Academies, Washington, DC.

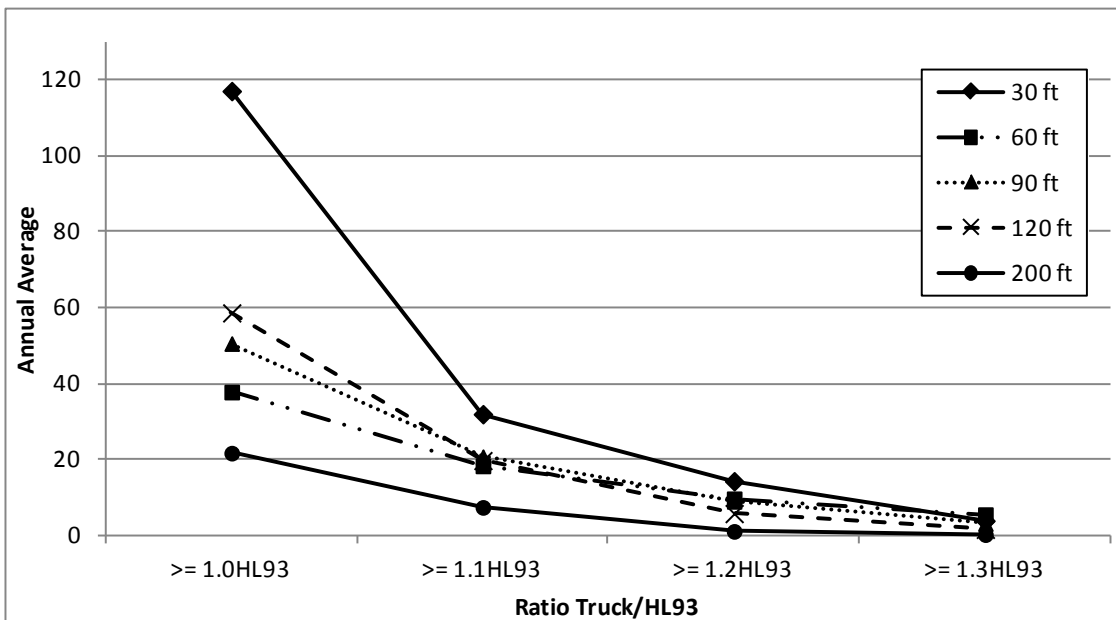
OTHER AFFECTED ARTICLES:

None

BACKGROUND:

This revision is a product of SHRP2 R19B, Bridges for Service Life Beyond 100 Years: Service Limit State Design which focused on calibration of Service Limit States in AASHTO LRFD similar to the calibration of the Strength

Limit State during the original development of AASHTO LRFD. In the case of this limit state often referred to as the design for overload there was found to be limited statistical data on the behavior under overload and little anecdotal evidence of damage in the field. It was possible to assess the frequency for which the current factored load was exceeded at 31 WIM sites with the results indicated in the figure below.



Annual average events scaled to ADTT=2500 versus ratio truck/HL-93.

A calibration using the WIM data (bias 1.35 and COV of 0.12 on HL93), uncertainties of dead load and flexural resistance from the original strength limit state calibration was applied to 41 bridges from the NCHRP 12-78 database and indicated that the reliability index for the limit state was higher than that found for the other service limit states investigated in R19B. The average reliability index determined using LFD requirements in place when this limit state was formulated was 1.8 for a single lane loaded and 1.6 for multiple lanes loaded. The corresponding COVs were 0.32 and 0.92, respectively. Monte Carlo simulations using one lane of 1.35 HL93 and the WIM statistics on load side and flexural resistance based on multiple lanes on the resistance side resulted in an average reliability index of 1.8 but a much reduced COV of 0.09. Discussions with owners indicated that the current design appears to be satisfying the perceived needs and provided a margin against possible future legal load increases under consideration. For more information see the R19B report at <http://www.trb.org/Main/Blurbs/170201.aspx>.

ANTICIPATED EFFECT ON BRIDGES:

None

REFERENCES:

See Background

OTHER:

None